Correlated electron systems periodically driven out of equilibrium: Floquet+DMFT formalism

Naoto Tsuji, Takashi Oka, and Hideo Aoki
Department of Physics, University of Tokyo, Hongo, Tokyo 113-0033, Japan
(Received 3 August 2008; revised manuscript received 28 November 2008; published 31 December 2008)

We propose to combine the Floquet formalism for systems in ac fields with the dynamical mean-field theory to study correlated electron systems periodically driven out of equilibrium by external fields such as intense laser light. This approach has a virtue that we can nonperturbatively include both the correlation effects and nonlinear effects due to the driving field, which is imperative in analyzing recent experiments for photoinduced phase transitions. In solving the problem, we exploit a general theorem that the Hamiltonian in a Floquet matrix form can be exactly diagonalized for single-band noninteracting systems. As a demonstration, we have applied the method to the Falicov-Kimball model in intense ac fields to calculate the spectral function. The result shows that photoinduced midgap states emerge from strong ac fields, triggering an insulator-metal transition.

DOI: 10.1103/PhysRevB.78.235124 PACS number(s): 71.27.+a, 78.20.Bh, 71.15.−m

I. INTRODUCTION

Controlling phases of matter is a central issue in the physics of strongly correlated electron systems, where a rich variety of phases are realized for various physical degrees of freedom such as spin and charge. Since a phase transition dramatically alters macroscopic properties of the system, it is of great importance to know how the phase changes as external parameters (temperature, pressure, band filling of the system, etc.) are varied, in equilibrium.

Now, the last decade witnessed that a controlling factor, intense laser fields, can trigger "phase transitions" in correlated electron materials.[1,2] One representative class of materials is perovskite manganites, in which an insulator-to-metal transition is induced by photoexcitation.[3,4] Recent experiments also indicate that a ferromagnetic spin alignment can emerge in the induced metallic phase in manganites.[5] Such phenomena are called photoinduced phase transitions (PIPTs), where irradiation of photons allows one to change electronic, magnetic, optical, or structural properties of the system.

The photoinduced phase transition, however, is distinct from conventional phase transitions in equilibrium in that the photon field drives the system out of equilibrium. In other words, the change in phases in nonequilibrium challenges our understanding of phase transitions which is normally conceived in equilibrium. In the PIPT, we have to consider, on top of the nonlinear electric-field effect, the electron correlation effect. The nonlinear effect appears as a threshold behavior, i.e., a macroscopic transition only occurs when the intensity of the driving field exceeds a certain strength. On the other hand, important correlation effects such as Mott's metal-insulator transition are nonperturbative effects. Thus, we cannot employ the linear-response theory[6] nor a mean-field treatment of the electron-electron interaction.

Here we propose a theoretical approach[7] for photoinduced phenomena, where the Floquet-Green function method (FGFM) (Refs. 8–11) is plugged into the dynamical mean-field theory (DMFT).[12] This formulation provides us with a promising way to treat both of the nonlinear effect of the electric field and the correlation effect simultaneously in a nonperturbative manner. We then apply the method to study the response of the Falicov-Kimball (FK) model,[13,14] one of the simplest lattice models for correlated electrons, to ac electric fields. A particular emphasis is put on the technical basis of FGFM.

During the preparation of the present study, we notice that Joura *et al.*[15] adopted a technique similar to FGFM to solve the Dyson equation for a system in dc fields. Here we present a general framework of DMFT out of equilibrium for *arbitrary time-periodic fields* in a more transparent viewpoint exploiting the Floquet formalism. In this context we should emphasize that FGFM is not just a numerical technique but offers a fruitful physical picture for nonequilibrium systems as revealed here.

The paper is organized as follows: in Sec. II, we review the Floquet theorem and the Floquet matrix method, on which our theoretical description is based. The rest of the paper is devoted to our original formulation. In Sec. III we define the Floquet matrix form of Green's function, which is our starting point of FGFM. Then in Sec. IV, we derive a general expression for Green's function and its inverse for noninteracting electrons in a Floquet matrix form. We calculate noninteracting Green's functions for several cases to discuss their physical implications. In Sec. V, we derive a general theorem that identifies the eigenvalues and the eigenvectors of a Floquet matrix form of the Hamiltonian for noninteracting electrons. While Secs. IV and V address noninteracting cases, we move on to correlated electron systems by incorporating FGFM in DMFT in Sec. VI. We formulate the obtained Green's function in a gauge-invariant manner in Sec. VII. We then apply our method to the FK model in Sec. VIII, and calculate the spectral functions for dc and ac fields, where we discuss how the Mott-insulating state is transformed into the metallic states in the external fields. We summarize the paper and give future problems in Sec. IX.

II. FLOQUET THEOREM AND FLOQUET MATRIX

An external field drives an electron having an energy ε into another state with a different energy, where there are many scattering channels in nonequilibrium. However, if the

driven system is periodic in time with a frequency Ω, the allowed channels are limited to the processes such that $\varepsilon \rightarrow \varepsilon + n\Omega$, where n is an integer. This greatly reduces the channels' degrees of freedom to be dealt with. One can take advantage of such a simplification through the Floquet matrix method,[16–18] of which we give an overview in this section.

The method has been used as an effective approach toward photoexcited systems. The concept of the Floquet matrix originates from the Floquet theorem[19] for a periodically driven system, an analog of the Bloch theorem applied to a spatially periodic system. Floquet theorem is a general theorem for differential equations of a form $dx(t)/dt = C(t)x(t)$ with C periodic in t, which include equations of motion for systems subject to external driving forces that periodically oscillate in time. One representative example is the Mathieu equation which describes a parametric resonance phenomenon. Here we restrict ourselves to a quantum system whose dynamics is determined by the time-dependent Schrödinger equation,

$$i\frac{d}{dt}\Psi(t) = H(t)\Psi(t), \tag{1}$$

where $\Psi(t)$ is a state vector of the system, and $H(t)$ is the time-dependent Hamiltonian, which is assumed to be periodic in t,

$$H(t+\tau) = H(t), \tag{2}$$

with a period τ. The Floquet theorem states that there exists a solution of Eq. (1) which is an eigenstate of the time translation operation $t \rightarrow t+\tau$, implying

$$\Psi_\alpha(t) = e^{-i\varepsilon_\alpha t}u_\alpha(t), \tag{3}$$

with $e^{-i\varepsilon_\alpha \tau}$ as an eigenvalue of the time translation, α as a set of quantum numbers, and $u_\alpha(t) = u_\alpha(t+\tau)$ as a periodic function of t. Hence we can Fourier expand $u_\alpha(t)$ as $u_\alpha(t) = \Sigma_n e^{-in\Omega t}u_\alpha^n$ with the frequency $\Omega = 2\pi/\tau$, where u_α^n is called the nth Floquet mode of Floquet state (3). We can then Fourier transform Eq. (1) to have

$$\sum_n H_{mn}u_\alpha^n = (\varepsilon_\alpha + m\Omega)u_\alpha^m, \tag{4}$$

where

$$H_{mn} \equiv \frac{1}{\tau}\int_{-\tau/2}^{\tau/2} dt e^{i(m-n)\Omega t}H(t) \tag{5}$$

is the Floquet matrix form of the Hamiltonian. The factor $\varepsilon_\alpha + m\Omega$ appearing on the right-hand side (rhs) of Eq. (4) is called *quasienergy*, which forms a ladder of energies with a spacing Ω. Since the Hamiltonian is time dependent, the energy is not conserved in general. However, Eq. (4) shows that the energy is conserved up to an integer multiple of Ω, corresponding to the absorption or emission of the photon with the energy Ω. Each element in the Floquet matrix H_{mn} corresponds to the probability amplitude of the transition from the mth Floquet mode to the nth one, so that off-diagonal components represent excitations driven by the external field while the diagonal ones the probability to remain in the same mode.

The consequence of the Floquet theorem is remarkable: Eq. (4) resembles the static Schrödinger equation in equilibrium except for the presence of the Floquet mode index n, which means that we have no longer to solve the time-dependent Schrödinger Eq. (1), in favor of the *time-independent* Eq. (4). This is the great advantage of the Floquet matrix method, which also plays a crucial role in Green's-function approach.

III. FLOQUET REPRESENTATION OF GREEN'S FUNCTION

Besides the Floquet analysis of the Hamiltonian, we can alternatively describe nonequilibrium states in Green's-function approach based on the Keldysh formalism.[20,21] The approach of the Floquet matrix proves its own worth when it is used within Green's-function formalism. The idea of FGFM was first introduced by Faisal,[8] followed by several groups.[9–11] In this section we give another way to define a Floquet matrix form of Green's function, which we shall use in this paper.

A Green's function has two independent arguments of time, t and t', as denoted by $G(t,t')$. We define variables $t_{\mathrm{rel}} \equiv t - t'$ and $t_{\mathrm{av}} \equiv (t+t')/2$. In equilibrium the system is invariant against continuous time translation, so that Green's functions depend on t and t' only through t_{rel}, which enables us to Fourier transform them into functions of ω. However, when the system is driven out of equilibrium, they generally depend on both t_{rel} and t_{av}. Since the periodic system that we consider in this paper has the discrete time translation invariance [Eq. (2)], it is guaranteed that Green's function is also invariant against $t_{\mathrm{av}} \rightarrow t_{\mathrm{av}} + \tau$. For an arbitrary function $G(t,t')$ (not limited to Green's function) that satisfies the periodicity condition, $G(t+\tau,t'+\tau) = G(t,t')$, we can define the Wigner transformation of G as

$$G_n(\omega) = \int_{-\infty}^{\infty} dt_{\mathrm{rel}} \frac{1}{\tau}\int_{-\tau/2}^{\tau/2} dt_{\mathrm{av}} e^{i\omega t_{\mathrm{rel}} + in\Omega t_{\mathrm{av}}} G(t,t'). \tag{6}$$

We call $G_n(\omega)$ the *Wigner representation* of the function G. Using the Wigner representation, we define the Floquet matrix form of G as

$$G_{mn}(\omega) \equiv G_{m-n}\left(\omega + \frac{m+n}{2}\Omega\right), \tag{7}$$

and call $G_{mn}(\omega)$ the *Floquet representation*. Hereafter a function with one index n should be understood as a Wigner representation, while two indices m and n mean a Floquet representation. In the Floquet representation, we use the reduced zone scheme, i.e., the range of ω is restricted to the "Brillouin zone" on the frequency axis: $-\Omega/2 < \omega \leq \Omega/2$. We can readily check that definition (7) is equivalent to the one given by Refs. 8–11. The Floquet representation is used during calculations, while the Wigner representation is used when we interpret the result since the Wigner representation has a clear physical interpretation that G_n is the nth oscillating mode in t_{av} of $G(t,t')$.

Actually, the Floquet representation $G_{mn}(\omega)$ has a one-to-one correspondence with the Wigner representation $G_\ell(\omega')$. $G_\ell(\omega') \to G_{mn}(\omega)$: the integers m and n should obey the conditions

$$m - n = \ell, \tag{8}$$

$$-\frac{\Omega}{2} < \omega' - \frac{m+n}{2}\Omega \leq \frac{\Omega}{2}, \tag{9}$$

for ℓ and ω'. There are two consecutive integers k and $k+1$ which can be equal to $m+n$ satisfying Eq. (9). Either k or $k+1$ is congruent to ℓ modulo 2. Thus $m+n$ is uniquely determined via Eq. (9) and the condition $m+n \equiv m-n \equiv \ell \pmod 2$. Together with Eq. (8), m and n are uniquely determined. For such m and n, ω is given by $\omega' - (m+n)\Omega/2$. $G_{mn}(\omega) \to G_\ell(\omega')$: ℓ and ω' are uniquely determined by $\ell = m-n$ and $\omega' = \omega + (m+n)\Omega/2$.

We can immediately realize the advantage of the Floquet representation in multiplications of two Floquet-represented functions. As shown in Appendix A, the mapping from $G(t,t')$ to $G_{mn}(\omega)$ preserves a multiplication structure,

$$\int dt'' A(t,t'')B(t'',t') = C(t,t')$$

$$\Leftrightarrow \sum_\ell A_{m\ell}(\omega)B_{\ell n}(\omega) = C_{mn}(\omega).$$

As an example, the Floquet representation of the Dyson equation is simplified into

$$(G_{\boldsymbol{k}})_{mn}(\omega) = (G^0_{\boldsymbol{k}})_{mn}(\omega) + \sum_{m'n'} (G^0_{\boldsymbol{k}})_{mm'}(\omega)(\Sigma_{\boldsymbol{k}})_{m'n'}(\omega) \times (G_{\boldsymbol{k}})_{n'n}(\omega), \tag{10}$$

where G and G^0 are, respectively, the full and the noninteracting Green's functions and Σ is the self-energy. Note that each function has the additional 2×2 matrix structure, $G = \begin{pmatrix} G^R & G^K \\ 0 & G^A \end{pmatrix}$ in the Keldysh space (with the three linearly independent components: the retarded, the advanced, and the Keldysh one). Thanks to the usual multiplication rule of the linear algebra, one can solve the Dyson Eq. (10) as $G_{\boldsymbol{k}}(\omega) = [G^{0^{-1}}_{\boldsymbol{k}}(\omega) - \Sigma_{\boldsymbol{k}}(\omega)]^{-1}$. In addition, a typical size of a Floquet matrix that is needed to be taken in numerical calculations is usually small because sufficiently high-order processes should tend to be irrelevant when the driving field is not so large, which also supports the usefulness of FGFM.

IV. NONINTERACTING ELECTRONS

Having defined the Floquet representation of Green's function in Eq. (7), we then compute the Floquet-represented Green's function for noninteracting electrons. Although FGFM has been used by several authors to study noninteracting electrons driven out of equilibrium, there are still further developments yet to be explored. This has motivated us to present an exact and unified description of FGFM that can be applied to general noninteracting single-band systems in this section.

In Sec. IV A we provide a general expression of the Floquet representation of Green's function for *any* single-band model. Then in Sec. IV B we derive the inverse of Green's function, which will be used to build DMFT in the Floquet matrix form in Sec. VI. After that, we show several examples of Green's function for the hypercubic (Sec. IV C) and other lattices (Sec. IV D). Throughout the paper we restrict our discussion to a single-band model, and omit spin degrees of freedom for simplicity.

A. General lattices and fields

Let $\epsilon_{\boldsymbol{k}}$ be a band dispersion of the system. We make the system subject to a homogeneous time-dependent electric field periodic in t. Here we choose the temporal gauge or the Hamiltonian gauge in which the scalar potential $\phi=0$. Replacing the momentum $\boldsymbol{k}$ with $\boldsymbol{k} - e\boldsymbol{A}(t)$ [$\boldsymbol{A}(t)$: a vector potential] in $\epsilon_{\boldsymbol{k}}$ gives the noninteracting Hamiltonian,

$$H(t) = \sum_{\boldsymbol{k}} \epsilon_{\boldsymbol{k}-e\boldsymbol{A}(t)} c^\dagger_{\boldsymbol{k}} c_{\boldsymbol{k}}, \tag{11}$$

where $c^\dagger_{\boldsymbol{k}}$ and $c_{\boldsymbol{k}}$ are the creation and the annihilation operators of the electrons, respectively, and we treat the electric field as a classical one. The retarded Green's function for noninteracting electrons reads

$$G^{R0}_{\boldsymbol{k}}(t,t') = -i\theta(t-t')\langle [c_{\boldsymbol{k}}(t), c^\dagger_{\boldsymbol{k}}(t')]_+ \rangle_0 = -i\theta(t-t')\exp\left(-i\int_{t'}^{t} dt''[\epsilon_{\boldsymbol{k}-e\boldsymbol{A}(t'')} - \mu]\right), \tag{12}$$

where $\theta(t)$ represents the step function, $[,]_+$ is the anticommutation relation, $\langle\cdots\rangle_0$ is the statistical average with respect to the initial density matrix $\rho_0 = e^{-\beta H(\boldsymbol{A}=0)}$ (where the system is assumed to be in equilibrium with the temperature β^{-1} at $t=-\infty$), and μ is the chemical potential of the system. We can transform Eq. (12) into the Wigner representation via Eq. (6), and then into the Floquet representation through Eq. (7). The details of the calculation are described in Appendix B. The final result is

$$(G^{R0}_{\boldsymbol{k}})_{mn}(\omega) = \sum_\ell \frac{1}{\omega + \ell\Omega + \mu - (\epsilon_{\boldsymbol{k}})_0 + i\eta} \times \int_{-\pi}^{\pi}\frac{dx}{2\pi}\int_{-\pi}^{\pi}\frac{dy}{2\pi} e^{i(m-\ell)x + i(\ell-n)y} \times \exp\left(-\frac{i}{\Omega}\int_y^x dz[\epsilon_{\boldsymbol{k}-e\boldsymbol{A}(z/\Omega)} - (\epsilon_{\boldsymbol{k}})_0]\right), \tag{13}$$

where η is a positive infinitesimal, and $(\epsilon_{\boldsymbol{k}})_0$ is the time-averaged dispersion, which coincides with the zeroth Floquet mode of $\epsilon_{\boldsymbol{k}}$,

$$(\epsilon_{\boldsymbol{k}})_{m-n} = \int_{-\pi}^{\pi}\frac{dz}{2\pi} e^{i(m-n)z}\epsilon_{\boldsymbol{k}-e\boldsymbol{A}(z/\Omega)}. \tag{14}$$

Equation (13) is the general Floquet representation of Green's function for the noninteracting system driven by a

periodic field. What is notable about expression (13) is that it can be decomposed into well-behaved matrices. Let us define two Floquet matrices,

$$(\Lambda_k)_{mn} = \int_{-\pi}^{\pi} \frac{dx}{2\pi} e^{i(m-n)x} \times \exp\left(-\frac{i}{\Omega}\int_0^x dz[\epsilon_{k-eA(z/\Omega)} - (\epsilon_k)_0]\right), \quad (15)$$

and

$$(Q_k)_{mn}(\omega) = \frac{1}{\omega + n\Omega + \mu - (\epsilon_k)_0 + i\eta}\delta_{mn}, \quad (16)$$

where Λ_k is unitary as shown in Appendix C, and $Q_k(\omega)$ is a diagonal matrix. The physical meaning of these matrices will be given later in Sec. V. Here let us just note a strikingly simple decomposition,

$$G_k^{R0}(\omega) = \Lambda_k \cdot Q_k(\omega) \cdot \Lambda_k^\dagger, \quad (17)$$

where we denote a multiplication of a Floquet matrix by " ·," and omit Floquet indices in Eq. (17). The decomposition [Eq. (17)] is essentially used to derive the inverse of Green's function in Sec. IV B.

The Floquet representation of the advanced Green's function is equal to the Hermitian adjoint of the retarded one: $(G_k^{A0})_{mn}(\omega) = (G_k^{R0^\dagger})_{mn}(\omega) = (G_k^{R0})^*_{nm}(\omega)$. Using Eq. (17), we have $G_k^{A0}(\omega) = \Lambda_k \cdot Q_k^\dagger(\omega) \cdot \Lambda_k^\dagger$.

B. Inverse of Green's function

When one solves a Dyson equation such as Eq. (10) to include effects of interaction, the noninteracting part appears as an inverse, $G_k^{R0^{-1}}(\omega)$, rather than $G_k^{R0}(\omega)$ itself. Using relation (17) and the unitarity of Λ_k, we can analytically invert Green's function as $G_k^{R0^{-1}}(\omega) = \Lambda_k \cdot Q_k^{-1}(\omega) \cdot \Lambda_k^\dagger$, which can be evaluated exactly as presented in Appendix D. The derived expression for the inverse of Green's function is

$$(G_k^{R0^{-1}})_{mn}(\omega) = (\omega + n\Omega + \mu + i\eta)\delta_{mn} - (\epsilon_k)_{m-n}. \quad (18)$$

One can also prove Eq. (18) from the Dyson equation for $G_k^{R0}(t,t')$ in a straightforward manner. Relation (18) means that Green's function is the kernel of Eq. (4), or that *the Floquet representation of Green's function is equivalent to the inverse of the Floquet matrix form of the quasienergy minus the Hamiltonian.* One can use Eq. (18) for *any* single-band Hamiltonian with a homogeneous electric field periodic in time. In Secs. IV C and IV D, we present examples of the calculations that utilize relation (18).

C. Hypercubic lattice

As a first example, let us consider a simple cubic lattice in d dimensions, whose energy dispersion is given by

$$\epsilon_k^{sc} = -2t\sum_{i=1}^{d} \cos k_i, \quad (19)$$

where t is the hopping and we set the lattice constant $a=1$. For simplicity we assume that the vector potential $\boldsymbol{A}(t)$ is parallel to $(1,1,\ldots,1)$ with each component $A_i(t)=A(t)$. Substituting k_i with $k_i - eA(t)$ in Eq. (19), we have

$$\epsilon_{k-eA(t)}^{sc} = \epsilon_k^{sc} \cos eA(t) + \bar{\epsilon}_k^{sc} \sin eA(t), \quad (20)$$

where we have defined

$$\bar{\epsilon}_k^{sc} = -2t\sum_{i=1}^{d} \sin k_i, \quad (21)$$

after Turkowski and Freericks.[22] Note that $\bar{\epsilon}_k^{sc}$ has the odd time-reversal symmetry. Every equation including ϵ_k^{sc} and $\bar{\epsilon}_k^{sc}$ must be consistent against the time-reversal operation. For instance, one usually finds the factor $\epsilon_k^{sc} + i\bar{\epsilon}_k^{sc}$, which is time-reversal even since the imaginary unit i is time-reversal odd.

An integral over $\boldsymbol{k}$ is performed through

$$\rho(\epsilon,\bar{\epsilon}) = \sum_k \delta(\epsilon - \epsilon_k^{sc})\delta(\bar{\epsilon} - \bar{\epsilon}_k^{sc}), \quad (22)$$

which is called the joint density of states (JDOS).[22] This contrasts with the equilibrium cases in which an integrand depends on $\boldsymbol{k}$ only through ϵ_k^{sc}, so that we can replace the integral variable $\boldsymbol{k}$ with ϵ_k^{sc} accompanied by the usual density of states $\rho(\epsilon)$. The analytic expression for JDOS in arbitrary d dimensions is summarized in Appendix E. In particular, in infinite dimensions the JDOS becomes a Gaussian function [Eq. (E2)].[22] In the following, we consider two kinds of electric fields, a dc field (Sec. IV C 1), and an ac field (Sec. IV C 2).

1. Hypercubic lattice in a dc field

A homogeneous dc field is given by the vector potential proportional to time,

$$eA(t)a = \Omega t, \quad (23)$$

where

$$\Omega = -eEa \quad (24)$$

is the Bloch frequency. The system with the field [Eq. (23)] fulfills the periodicity condition [Eq. (2)] with the period $2\pi/\Omega$ because of the periodic potential of the lattice. With Eq. (13), Green's function has the following Floquet representation,

$$(G_k^{R0})_{mn}(\omega) = e^{i(m-n)\theta_k}\sum_\ell \frac{1}{\omega + \ell\Omega + \mu + i\eta} \times J_{m-\ell}\left(\frac{\zeta_k}{\Omega}\right)J_{\ell-n}\left(\frac{\zeta_k}{\Omega}\right), \quad (25)$$

where $J_n(z)$ is the nth-order Bessel function, and

$$\zeta_k = \sqrt{(\epsilon_k^{sc})^2 + (\bar{\epsilon}_k^{sc})^2}, \quad (26)$$

$$\tan\theta_k = \bar{\epsilon}_k^{sc}/\epsilon_k^{sc}. \quad (27)$$

To see how Green's function (25) behaves, we calculate the local spectral function $A_n(\omega) = -\frac{1}{\pi}\mathrm{Im}\,\Sigma_k(G_k^{R0})_n(\omega)$ in infinite dimensions. First, we transform Eq. (25) into the Wigner representation, and then integrate it over $\boldsymbol{k}$ with the JDOS

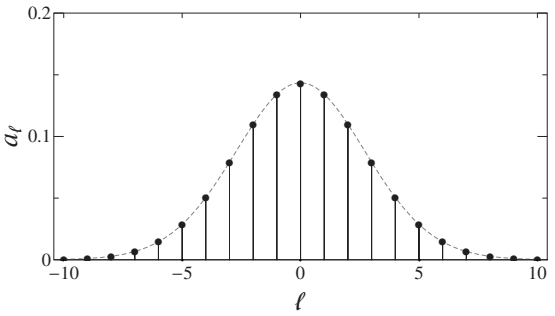

FIG. 1. The coefficients a_ℓ of the delta functions in the local spectral function of the noninteracting electrons on the hypercubic lattice with the dc field $\Omega=0.25$ are plotted by the circles. The delta functions with the spacing Ω are schematically shown by the solid lines. The broken line is a guide for the eyes.

[Eq. (E2)]. After taking the imaginary part, we arrive at

$$A_n(\omega) = \delta_{n,0} \sum_\ell a_\ell \delta(\omega + \ell\Omega + \mu). \tag{28}$$

Here the coefficients in front of the delta functions are $a_\ell = e^{-1/2\Omega^2} I_\ell(1/2\Omega^2)$, where $I_\ell(z)$ is the modified Bessel function of the first kind. Note that the coefficients satisfy the normalization condition, $\Sigma_\ell a_\ell = 1$.

Equation (28) shows that the local spectral function has only the $n=0$ component, indicating that the spectral function evolves into a time-independent function [Eq. (28)] for a sufficiently long time elapsed after the dc field began to drive the system.[22] Later in Sec. VII A, we shall show that the components with $n \neq 0$ vanish due to a symmetry in the system.

The spectral function on the hypercubic lattice, displayed in Fig. 1, consists of a set of delta functions with a spacing Ω, namely, the Wannier-Stark ladder. The width of each peak (approximately effective hopping) is infinitesimal due to the Bloch oscillation, where an electron is not free to run in a lattice, but only oscillates with the frequency Ω.

The inverse of the Floquet-represented Green's function in this case is given via relation (18) by

$$\begin{aligned}(G_{\boldsymbol{k}}^{R0^{-1}})_{mn}(\omega) &= (\omega + n\Omega + \mu + i\eta)\delta_{mn} \\ &\quad - \frac{1}{2}[(\epsilon_{\boldsymbol{k}}^{\mathrm{sc}} + i\bar{\epsilon}_{\boldsymbol{k}}^{\mathrm{sc}})\delta_{m-n,1} + (\epsilon_{\boldsymbol{k}}^{\mathrm{sc}} - i\bar{\epsilon}_{\boldsymbol{k}}^{\mathrm{sc}})\delta_{m-n,-1}] \\ &= (\omega + n\Omega + \mu + i\eta)\delta_{mn} \\ &\quad - \frac{1}{2} e^{i(m-n)\theta_{\boldsymbol{k}}} \zeta_{\boldsymbol{k}} (\delta_{m-n,1} + \delta_{m-n,-1}).\end{aligned} \tag{29}$$

The Hamiltonian part of Eq. (29) is explicitly written down in a tridiagonal matrix form as

$$\frac{1}{2}\begin{pmatrix} \ddots & \ddots & & & & & \\ \ddots & 0 & \zeta_{\boldsymbol{k}} e^{i\theta_{\boldsymbol{k}}} & & & 0 & \\ & \zeta_{\boldsymbol{k}} e^{-i\theta_{\boldsymbol{k}}} & 0 & \zeta_{\boldsymbol{k}} e^{i\theta_{\boldsymbol{k}}} & & & \\ & & \zeta_{\boldsymbol{k}} e^{-i\theta_{\boldsymbol{k}}} & 0 & \zeta_{\boldsymbol{k}} e^{i\theta_{\boldsymbol{k}}} & & \\ & & & \zeta_{\boldsymbol{k}} e^{-i\theta_{\boldsymbol{k}}} & 0 & \zeta_{\boldsymbol{k}} e^{i\theta_{\boldsymbol{k}}} & \\ & 0 & & & \zeta_{\boldsymbol{k}} e^{-i\theta_{\boldsymbol{k}}} & 0 & \ddots \\ & & & & & \ddots & \ddots \end{pmatrix}. \tag{30}$$

As remarked in Sec. II, each component of the Floquet matrix [Eq. (30)] represents a probability amplitude of a transition from one Floquet mode to another. Note that for the case of the dc field, Hamiltonian (30) has no diagonal components, which means that the electrons cannot stay stationary but are always excited by the field. We also note that the off diagonal components do not depend on Ω which is proportional to the strength of the field. The dependence of Ω is only taken into account through the quasienergy part of Eq. (29).

2. Hypercubic lattice in an ac field

Let us move on to the case of the ac field on the hypercubic lattice. The vector potential is defined by

$$eA(t)a = A \sin \Omega t, \tag{31}$$

where Ω is the frequency of the ac field, and

$$A = -\frac{eEa}{\Omega} \tag{32}$$

is its amplitude divided by the frequency. Although we use the symbol Ω, this should not be confused with Ω (the Bloch frequency) introduced in Eq. (24) for the dc field. Following Eq. (13), we derive the Floquet representation of Green's function as

$$\begin{aligned}(G_{\boldsymbol{k}}^{R0})_{mn}(\omega) &= \sum_\ell \frac{1}{\omega + \ell\Omega + \mu - \epsilon_{\boldsymbol{k}}^{\mathrm{sc}} J_0(A) + i\eta} \\ &\quad \times \int_{-\pi}^{\pi} \frac{dx}{2\pi} \int_{-\pi}^{\pi} \frac{dy}{2\pi} e^{i(m-\ell)x + i(\ell-n)y} \\ &\quad \times \exp\left(-\frac{i}{\Omega} \int_y^x dz \{ \epsilon_{\boldsymbol{k}}^{\mathrm{sc}} [\cos(A \sin z) - J_0(A)] \right. \\ &\quad \left. + \bar{\epsilon}_{\boldsymbol{k}}^{\mathrm{sc}} \sin(A \sin z) \} \right).\end{aligned} \tag{33}$$

Taking the imaginary part of Eq. (33) and integrating over $\boldsymbol{k}$ with the JDOS [Eq. (E2)], we obtain the local spectral function. We depict it for several A and $\Omega=1$ in Fig. 2. One can see that the spectral function has narrow peaks at $\omega = n\Omega$ ($n=0, \pm 1, \pm 2, \ldots$) known as the *dynamical Wannier-Stark ladder*. The peaks at $\omega = \pm\Omega$ correspond to one-photon absorption or emission, and the peaks at $\omega = \pm 2\Omega$ correspond to a two-photon one, etc. The width of each peak, or the effective hopping, is renormalized by the zeroth-order Bessel function $J_0(A)$ as seen in Eq. (33), and even vanishes making

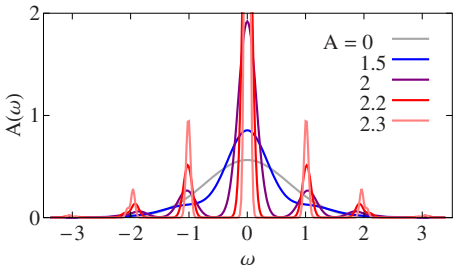

FIG. 2. (Color online) The local spectral functions of the noninteracting electrons on the hypercubic lattice coupled to the ac field with $\Omega=1$ and $A=0$, 1.5, 2, 2.2, and 2.3.

the electrons completely localized when $J_0(A)=0$. In Fig. 2 one finds that the widths of the peaks shrink as A approaches the first zero ($z=2.404\,83\cdots$) of $J_0(A)$ until finally the peaks become the delta functions. This scaling has been known as *dynamical localization* since the proposal by Dunlap and Kenkre.[23]

The inverse of Green's function in the ac field can be calculated via Eq. (18). The result is

$$(G_{\boldsymbol{k}}^{R0^{-1}})_{mn}(\omega) = (\omega + n\Omega + \mu + i\eta)\delta_{mn} - \begin{cases} \epsilon_{\boldsymbol{k}}^{\mathrm{sc}} J_{m-n}(A), & m-n: \text{ even} \\ i\bar{\epsilon}_{\boldsymbol{k}}^{\mathrm{sc}} J_{m-n}(A), & m-n: \text{ odd}. \end{cases} \tag{34}$$

The explicit Floquet matrix form of the Hamiltonian part of Eq. (34) reads

$$\begin{pmatrix} \ddots & & \vdots & & & & \\ & \epsilon_{\boldsymbol{k}}J_0(A) & i\bar{\epsilon}_{\boldsymbol{k}}J_1(A) & \epsilon_{\boldsymbol{k}}J_2(A) & i\bar{\epsilon}_{\boldsymbol{k}}J_3(A) & \epsilon_{\boldsymbol{k}}J_4(A) & \\ & -i\bar{\epsilon}_{\boldsymbol{k}}J_1(A) & \epsilon_{\boldsymbol{k}}J_0(A) & i\bar{\epsilon}_{\boldsymbol{k}}J_1(A) & \epsilon_{\boldsymbol{k}}J_2(A) & i\bar{\epsilon}_{\boldsymbol{k}}J_3(A) & \\ \cdots & \epsilon_{\boldsymbol{k}}J_2(A) & -i\bar{\epsilon}_{\boldsymbol{k}}J_1(A) & \epsilon_{\boldsymbol{k}}J_0(A) & i\bar{\epsilon}_{\boldsymbol{k}}J_1(A) & \epsilon_{\boldsymbol{k}}J_2(A) & \cdots \\ & -i\bar{\epsilon}_{\boldsymbol{k}}J_3(A) & \epsilon_{\boldsymbol{k}}J_2(A) & -i\bar{\epsilon}_{\boldsymbol{k}}J_1(A) & \epsilon_{\boldsymbol{k}}J_0(A) & i\bar{\epsilon}_{\boldsymbol{k}}J_1(A) & \\ & \epsilon_{\boldsymbol{k}}J_4(A) & -i\bar{\epsilon}_{\boldsymbol{k}}J_3(A) & \epsilon_{\boldsymbol{k}}J_2(A) & -i\bar{\epsilon}_{\boldsymbol{k}}J_1(A) & \epsilon_{\boldsymbol{k}}J_0(A) & \\ & & \vdots & & & & \ddots \end{pmatrix}, \tag{35}$$

where we omit the label "sc" attached to $\epsilon_{\boldsymbol{k}}$ and $\bar{\epsilon}_{\boldsymbol{k}}$ for simplicity. Taking the dc limit $\Omega\to 0$ requires a special care because of definition (32) which is singular at $\Omega=0$. Therefore a quantity calculated for a system in the presence of the ac field with a finite frequency $\Omega\neq 0$ does not necessarily reproduce the result calculated for a system with the dc field discussed in Sec. IV C 1.

Let us examine the physical meaning of the Floquet matrix [Eq. (35)]. The (m,n) component of Hamiltonian (35) is proportional to $J_{m-n}(A)$. Since $J_{m-n}(A)\propto A^{|m-n|}$ if A is sufficiently small, the transition probability $m\to n$ is proportional to $E^{2|m-n|}$. For $m<n$, the process corresponds to stimulated absorption, while it corresponds to stimulated emission for $m>n$. The process of spontaneous emission is not included since we assume that the electric field is classical so that there is no quantum fluctuation of photon numbers. This assumption is appropriate as long as the intensity of the electric field considered here be so strong as a pulsed laser.

D. Application to other lattices

So far we have assumed that the vector potential $\boldsymbol{A}$ points to the specific direction $(1,1,\ldots,1)$ in the hypercubic lattice. We can more generally calculate the inverse of the noninteracting retarded Green's function $G^{R0^{-1}}$ by making use of formula (18) for arbitrary lattice structures and the vector potentials. The disadvantage of such a general case is that, since the $\boldsymbol{k}$ dependence of $G^{R0^{-1}}$ is not so simple as to be only through $\epsilon_{\boldsymbol{k}}^{\mathrm{sc}}$ and $\bar{\epsilon}_{\boldsymbol{k}}^{\mathrm{sc}}$, the integral over $\boldsymbol{k}$ becomes computationally heavier.

Here we note that there is a group of lattice models that give a simple $\boldsymbol{k}$-dependence of $G^{R0^{-1}}$ in infinite dimensions. Among them are the face-centered cubic (fcc) (Sec. IV D 1) and body-centered cubic (bcc) (Sec. IV D 2) lattices with $\boldsymbol{A}$ parallel to $(1,1,\ldots,1)$ in infinite dimensions. It is instructive to give examples other than the hypercubic lattice.

1. fcc lattice in infinite dimensions

The energy dispersion of the fcc lattice generalized to arbitrary d dimensions ($d\geq 2$) is given by

$$\epsilon_{\boldsymbol{k}}^{\mathrm{fcc}} = \frac{4}{2\sqrt{d(d-1)}} \sum_{\alpha=2}^{d} \sum_{\beta=1}^{\alpha-1} \cos k_\alpha \cos k_\beta. \tag{36}$$

In the infinite-dimensional limit ($d\to\infty$) the dispersion of the fcc lattice $\epsilon_{\boldsymbol{k}}^{\mathrm{fcc}}$ is related to that for the sc lattice [Eq. (19)] through,[24]

$$\epsilon_{\boldsymbol{k}}^{\mathrm{fcc}} = (\epsilon_{\boldsymbol{k}}^{\mathrm{sc}})^2 - \frac{1}{2}. \tag{37}$$

Using Eqs. (18) and (37), we derive the inverse of Green's function for the infinite-dimensional fcc lattice in the dc field,

$$(G_{\boldsymbol{k}}^{R0^{-1}})_{mn}(\omega) = (\omega + n\Omega + \mu + i\eta)\delta_{mn} - \frac{1}{4}e^{i(m-n)\theta_{\boldsymbol{k}}}[\zeta_{\boldsymbol{k}}^2(\delta_{m-n,2} + \delta_{m-n,-2}) + 2(\zeta_{\boldsymbol{k}}^2 - 1)\delta_{mn}]. \tag{38}$$

We see that the Hamiltonian part of the inverse of Green's function [the second term on the rhs of Eq. (38)] is written in a pentadiagonal matrix form. In the same way we can obtain Green's function on the ac field via Eq. (18). The result reads

$$(G_{\boldsymbol{k}}^{R0^{-1}})_{mn}(\omega) = (\omega + n\Omega + \mu + i\eta)\delta_{mn} - \frac{1}{2}\begin{cases} \zeta_{\boldsymbol{k}}^2 \cos(2\theta_{\boldsymbol{k}})J_{m-n}(2A) + (\zeta_{\boldsymbol{k}}^2 - 1)\delta_{mn}, & m-n: \text{ even} \\ i\zeta_{\boldsymbol{k}}^2 \sin(2\theta_{\boldsymbol{k}})J_{m-n}(2A), & m-n: \text{ odd}. \end{cases} \tag{39}$$

We notice that the factors $J_{m-n}(2A)$ and $J_{m-n}(0)=\delta_{mn}$ appear in Eq. (39) [while $J_{m-n}(A)$ appears on the sc lattice; see Eq. (34)]. Equations (38) and (39) indicate that Green's functions depend on $\boldsymbol{k}$ only via the two functions $\epsilon_{\boldsymbol{k}}^{\mathrm{sc}}$ [Eq. (19)] and $\bar{\epsilon}_{\boldsymbol{k}}^{\mathrm{sc}}$ [Eq. (21)], so that we can integrate over $\boldsymbol{k}$ using the JDOS [Eq. (22)].

2. bcc lattice in infinite dimensions

The bcc lattice in d dimensions ($d \geq 3$) is defined by the dispersion relation,

$$\epsilon_{\boldsymbol{k}}^{\mathrm{bcc}} = -\frac{8}{2\sqrt{d(d-1)(d-2)}}\sum_{\alpha=3}^{d}\sum_{\beta=2}^{\alpha-1}\sum_{\gamma=1}^{\beta-1}\cos k_\alpha \cos k_\beta \cos k_\gamma. \tag{40}$$

We can take the limit $d \to \infty$ in the same way as in the case of the fcc lattice, and the dispersion converges to

$$\epsilon_{\boldsymbol{k}}^{\mathrm{bcc}} = \frac{2}{3}(\epsilon_{\boldsymbol{k}}^{\mathrm{sc}})^3 - \epsilon_{\boldsymbol{k}}^{\mathrm{sc}}, \tag{41}$$

from which we can derive Green's function in the dc field,

$$(G_{\boldsymbol{k}}^{R0^{-1}})_{mn}(\omega) = (\omega + n\Omega + \mu + i\eta)\delta_{mn} - \frac{1}{12}e^{i(m-n)\theta_{\boldsymbol{k}}}\zeta_{\boldsymbol{k}}[\zeta_{\boldsymbol{k}}^2(\delta_{m-n,3} + \delta_{m-n,-3}) + 3(\zeta_{\boldsymbol{k}}^2 - 2)(\delta_{m-n,1} + \delta_{m-n,-1})]. \tag{42}$$

In this case the Hamiltonian part of the inverse of Green's function [the second term on the rhs of Eq. (42)] becomes a heptadiagonal matrix. Similarly, Green's function in the ac field is written as

$$(G_{\boldsymbol{k}}^{R0^{-1}})_{mn}(\omega) = (\omega + n\Omega + \mu + i\eta)\delta_{mn} - \frac{1}{6}\begin{cases} \zeta_{\boldsymbol{k}}[\zeta_{\boldsymbol{k}}^2 \cos(3\theta_{\boldsymbol{k}})J_{m-n}(3A) + 3(\zeta_{\boldsymbol{k}}^2 - 2)\cos\,\theta_{\boldsymbol{k}}J_{m-n}(A)], & m-n: \text{ even} \\ i\zeta_{\boldsymbol{k}}[\zeta_{\boldsymbol{k}}^2 \sin(3\theta_{\boldsymbol{k}})J_{m-n}(3A) + 3(\zeta_{\boldsymbol{k}}^2 - 2)\sin\,\theta_{\boldsymbol{k}}J_{m-n}(A)], & m-n: \text{ odd}, \end{cases} \tag{43}$$

where the factor $J_{m-n}(3A)$ newly appears besides $J_{m-n}(A)$. Again, Green's functions depend on $\boldsymbol{k}$ only through $\epsilon_{\boldsymbol{k}}^{\mathrm{sc}}$ and $\bar{\epsilon}_{\boldsymbol{k}}^{\mathrm{sc}}$, which makes an integral over $\boldsymbol{k}$ computationally quite efficient with the JDOS [Eq. (22)].

V. DIAGONALIZATION OF FLOQUET MATRICES

Here we examine how to diagonalize a Floquet matrix $(\omega+n\Omega)\delta_{mn}-H_{mn}$ appearing in the original Schrödinger Eq. (4) for the noninteracting electrons. We have shown in Sec. IV A that the Floquet matrix form of Green's function is diagonalized into $Q_{\boldsymbol{k}}(\omega)$ by the unitary transformation $\Lambda_{\boldsymbol{k}}$ [see Eq. (17)]. In Sec. IV B, we have mentioned that the inverse of Green's function is equivalent to the Floquet matrix $(\omega+n\Omega+\mu+i\eta)\delta_{mn}-H_{mn}$. Combining these two facts, we identify the eigenvalues and the eigenvectors of the Floquet matrix. We summarize the statement below.

The eigenvalues of a Floquet matrix $H_{mn}-n\Omega\delta_{mn}$ for a single-band noninteracting system subject to a homogeneous electric field periodic in time are

$$-(Q_{\boldsymbol{k}}^{-1})_{nn}(0) = (\epsilon_{\boldsymbol{k}})_0 - n\Omega = H_{nn} - n\Omega \quad (n = 0, \pm 1, \pm 2, \ldots), \tag{44}$$

and for each n, the corresponding eigenvector is given by

$$u_{\boldsymbol{k}}^{m-n} = (\Lambda_{\boldsymbol{k}})_{mn} \quad (m = 0, \pm 1, \pm 2, \ldots). \tag{45}$$

This completely solves Floquet matrix problems for a single-band system of noninteracting electrons. We note that the fact that Eq. (44) gives the eigenvalues is essentially a consequence of Shirley's relation [Eq. (5) of Ref. 16]. Since $(\epsilon_{\boldsymbol{k}})_0\tau$ is a dynamical phase, the above statement indicates the absence of an additional geometrical phase (see Appendix D).

From Eqs. (17) and (45), the noninteracting Green's function can be written with the Floquet states as

$$(G_{\boldsymbol{k}}^{R0})_{mn}(\omega) = \sum_{\ell}\frac{u_{\boldsymbol{k}}^{m-\ell}(u_{\boldsymbol{k}}^{n-\ell})^*}{\omega + \ell\Omega + \mu - (\epsilon_{\boldsymbol{k}})_0 + i\eta}. \tag{46}$$

One should note that the theorem cannot be applied to a multiband system, where contributions of a geometrical phase may survive and interband transition could be caused by the electric field.

The theorem provides a unified description of periodically driven systems: the original band structure $\epsilon_{\boldsymbol{k}}$ is renormalized into the time-averaged one $(\epsilon_{\boldsymbol{k}})_0$ due to the field, and the renormalized band splits into its *replicas* with the spacing Ω. On the (hyper)cubic lattice, the dc field changes the band into the Wannier-Stark ladder with the infinitesimal band-

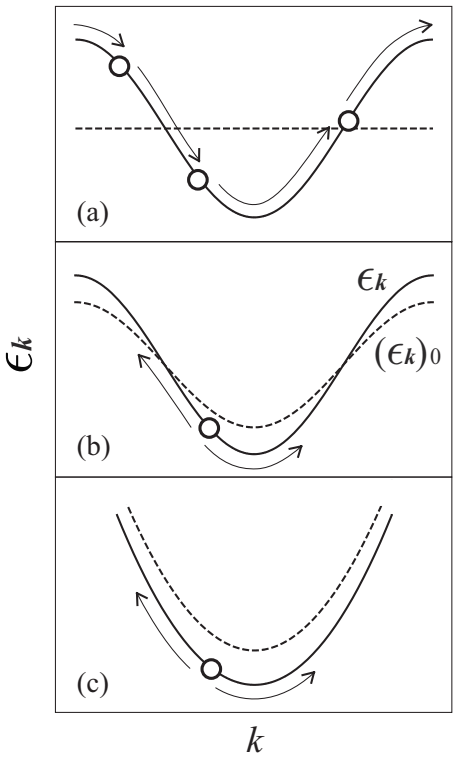

FIG. 3. The band renormalization $\epsilon_{\boldsymbol{k}} \rightarrow (\epsilon_{\boldsymbol{k}})_0$ on the (hyper)cubic lattice in (a) the dc field and (b) the ac field and (c) on a parabolic band in the ac field. The solid line represents $\epsilon_{\boldsymbol{k}}$, while the dashed line represents $(\epsilon_{\boldsymbol{k}})_0$. The circles are occupied states moving along the arrows.

width [Fig. 3(a)], while in the ac field, the bandwidth scales with the factor $J_0(A)$ [Fig. 3(b)].

To see how the theorem actually works, let us apply it to the d-dimensional fcc lattice model in the dc field as an example. For convenience, we restrict our discussion in the limit $d \rightarrow \infty$. The Floquet matrix form of the Hamiltonian is given by Eq. (38). According to the theorem, its eigenvalues are equal to the diagonal components: $\omega + n\Omega - \frac{1}{2}(\zeta_{\boldsymbol{k}}^2 - 1)$. This means that the dc field modifies the energy dispersion from $\epsilon_{\boldsymbol{k}}^{\mathrm{fcc}}$ [Eq. (37)] to $\tilde{\epsilon}_{\boldsymbol{k}}^{\mathrm{fcc}} \equiv \frac{1}{2}(\zeta_{\boldsymbol{k}}^2 - 1)$. The latter dispersion is equivalent to the one for a $(d-1)$-dimensional hyperplane perpendicular to $(1,1,\ldots,1)$, the direction of the electric field. We can interpret this fact as follows: the dc field makes the electrons localize along the direction of the field due to the Bloch oscillation, but the electrons are free to move along the directions perpendicular to the field because along those directions the force of the dc field does not act on the electrons. As a result, the motion of the electrons is confined on the hyperplane, and the energy dispersion becomes $\tilde{\epsilon}_{\boldsymbol{k}}^{\mathrm{fcc}}$.

Another example is provided by an ac field. If one sees the Floquet matrix form of the Hamiltonian for the system in an ac field on the fcc [Eq. (39)] or bcc [Eq. (43)] lattices, one finds that various kinds of band renormalization besides the $J_0(A)$ scaling on the simple cubic lattice are implied by the theorem.

Finally, let us consider electrons in a parabolic band (e.g., a conduction-band bottom in a semiconductor) with $\epsilon_{\boldsymbol{k}} = \boldsymbol{k}^2/2m^*$. If we apply an ac field on it, the dispersion is renormalized into $(\epsilon_{\boldsymbol{k}})_0 = \epsilon_{\boldsymbol{k}} + e^2E^2/4m^*\Omega^2$ [Fig. 3(c)]. This results from the dynamical Franz-Keldysh effect,[25,26] which is, in the present formalism, naturally understood through the diagonalization picture of the Floquet matrix.

VI. DYNAMICAL MEAN-FIELD THEORY WITH THE FLOQUET-GREEN FUNCTION METHOD

Now we are in position to combine FGFM with DMFT for treating interacting systems in external fields. At the basis of DMFT lies the fact that a lattice problem of correlated many-body systems can be approximately mapped to a problem of an impurity embedded into the environment of an effective medium when one ignores spatial fluctuations but takes fully into account on-site dynamical correlation.[12,27] The mapping is given as follows: let $Z = \int [dc_i][dc_i^\dagger] e^{iS[c_i, c_i^\dagger]}$ be a partition function in terms of the original action, $S = \int dt \int dt' \Sigma_{ij} c_i^\dagger(t) G_{ij}^{0^{-1}}(t,t') c_j(t') + \Sigma_i S_{\mathrm{int}}[c_i, c_i^\dagger]$, where the interaction term is assumed to be a sum of the local terms. Integrating out each site's degrees of freedom except for a representative site $i=o$, we have the local partition function $Z_{\mathrm{loc}}[\mathcal{G}_0] = \int [dc_o][dc_o^\dagger] e^{iS_{\mathrm{loc}}[c_o, c_o^\dagger]}$. Here the local action reads $S_{\mathrm{loc}} = \int dt \int dt' c_o^\dagger(t) \mathcal{G}_0^{-1}(t,t') c_o(t') + S_{\mathrm{int}}[c_o, c_o^\dagger]$ [$\mathcal{G}_0(t,t')$: the Weiss function]. If one ignores the nonlocal fluctuations, Z and Z_{loc} give a common site-diagonal self-energy, $\Sigma_{ij}(t,t') = \delta_{ij}\Sigma(t,t')$. This fact enables us to build a set of self-consistent closed equations, which can be solved with an iterative numerical calculation. Although neglecting the spatial fluctuation is generally an approximation, the nonlocal corrections become rigorously irrelevant in the limit of infinite dimensions, where the hopping parameter is scaled as $t = t^*/2\sqrt{d}$ (t^*: fixed).[28]

DMFT is also applicable to nonequilibrium systems as recently studied[29–31] based on nonequilibrium Green's-function formalism. Similar to the equilibrium case, one has self-consistent equations for Green's function and the self-energy. Now, the present proposal is that if the driven system is periodic in time, one can rewrite the equations in the Floquet matrix form,

$$(G_{\mathrm{loc}})_{mn}(\omega) = \frac{\delta Z_{\mathrm{loc}}[\mathcal{G}_0]}{\delta(\mathcal{G}_0^{-1})_{nm}(\omega)}, \tag{47}$$

$$(G_{\mathrm{loc}}^{-1})_{mn}(\omega) = (\mathcal{G}_0^{-1})_{mn}(\omega) - \Sigma_{mn}(\omega), \tag{48}$$

$$(G_{\boldsymbol{k}}^{-1})_{mn}(\omega) = (G_{\boldsymbol{k}}^{0^{-1}})_{mn}(\omega) - \Sigma_{mn}(\omega), \tag{49}$$

$$(G_{\mathrm{loc}})_{mn}(\omega) = \sum_{\boldsymbol{k}} (G_{\boldsymbol{k}})_{mn}(\omega). \tag{50}$$

To solve Eqs. (47)–(50) self-consistently, we first input the inverse of the noninteracting Green's function given by Eq. (18) into Eq. (49). After the initial self-energy is properly chosen, the calculation is iterated until Green's function converges. For the lattices discussed in Secs. IV C and IV D, the integral over $\boldsymbol{k}$ in Eq. (50) is performed via the JDOS [Eq. (22)]. As remarked in Sec. III, the size of the Floquet matrix that needs to be taken in a calculation is usually small

(~5–30, depending on Ω), which, with the analytic expression of the inverse of Green's function (18), makes our computational costs dramatically small.

VII. GAUGE-INVARIANT GREEN'S FUNCTION

Before applying our method to a model, we examine the gauge invariance of Green's function. Let us write the coordinates $x^\nu=(t,\boldsymbol{r})$ and the vector potential $A^\nu=(\phi,\boldsymbol{A})$ in the four-vector form. The gauge transformation, $A_\nu(x)\to A_\nu(x)+\partial_\nu\chi(x)$, puts a phase factor to the creation and the annihilation operators as $c^\dagger(x)\to e^{-ie\chi(x)}c^\dagger(x)$ and $c(x)\to e^{ie\chi(x)}c(x)$. Accordingly Green's function changes as $G(x,x')\to e^{ie[\chi(x)-\chi(x')]}G(x,x')$, i.e., the usual Green's function is not gauge invariant. It is known[32,33] that one can make Green's function gauge invariant with an additional phase factor as

$$\tilde{G}(x,x')=\exp\left(-i\int_{x'}^{x}dy^\nu eA_\nu(y)\right)G(x,x'). \tag{51}$$

$\tilde{G}$ depends on the path of the line integral in the exponent. Here we adopt the conventional straight line connecting x with x' as the path of the integral. Suppose that Green's function depends on $\boldsymbol{k}$ only through $\epsilon_{\boldsymbol{k}}^{\mathrm{sc}}$ and $\bar{\epsilon}_{\boldsymbol{k}}^{\mathrm{sc}}$. Then in the temporal gauge ($\phi=0$) the Wigner representation of the modified Green's function $\tilde{G}$ becomes

$$\begin{aligned}\tilde{G}_m(\zeta,\theta,\omega)=\sum_n\int\frac{d\omega'}{2\pi}\frac{1}{\tau}\int_{-\tau/2}^{\tau/2}dt_{\mathrm{av}}\int dt_{\mathrm{rel}}\\ \times e^{i(m-n)\Omega t_{\mathrm{av}}+i(\omega-\omega')t_{\mathrm{rel}}}\\ \times G_n\left(\zeta,\theta+\int_{-1/2}^{1/2}d\lambda eA(t_{\mathrm{av}}+\lambda t_{\mathrm{rel}}),\omega'\right),\end{aligned} \tag{52}$$

where ζ and θ are defined in Eqs. (26) and (27). Note that $\tilde{G}$ is calculated by shifting the variable θ in the original Green's function. This suggests that Green's function integrated in terms of θ is definitely gauge invariant, so that the local Green's function $\Sigma_{\boldsymbol{k}}G_{\boldsymbol{k}}(\omega)$ is also gauge invariant.[33] In the following, we derive the gauge-invariant Green's function $\tilde{G}$ for the dc field in Sec. VII A and the ac field in Sec. VII B.

A. dc field

To obtain $\tilde{G}$ for the dc field, we first note that the Hamiltonian in the dc field [Eq. (23)] has the time translation symmetry. If one makes a time translation $t\to t+\delta t$, the vector potential changes as $A(t)\to A(t)+\Omega\delta t$. Since the change can be absorbed by the gauge transformation with $\chi=-\Omega\delta t\Sigma_{i=1}^{d}x^i$, the Hamiltonian is invariant against time translation. Then we *assume* that in the long-time limit after the dc field is switched on the retarded Green's function becomes independent of the initial correlations. This assumption seems to be valid[34] as numerically checked in Sec. VIII A. As a result, a gauge-invariant quantity that is calculated from the retarded Green's function should be independent of the average time t_{av}. For instance, the local Green's function in the Wigner representation $(G_{\mathrm{loc}}^R)_n(\omega)$, which is gauge invariant as shown above, vanishes for $n\neq 0$, so that $G_{\mathrm{loc}}^R(t,t')$ does not depend on t_{av}. In the same way the self-energy $\Sigma_n^R(\omega)$ also vanishes for $n\neq 0$.

Since the Floquet-represented self-energy $\Sigma_{mn}^R(\omega)$ is diagonal due to the symmetry, we can identify the θ dependence of the Floquet representation of the retarded Green's function as

$$G_{mn}^R(\zeta,\theta,\omega)=e^{i(m-n)\theta}G_{mn}^R(\zeta,\theta=0,\omega). \tag{53}$$

Using Eq. (53), one can evaluate the gauge-invariant Green's function (52) as

$$\tilde{G}_m^R(\zeta,\theta,\omega)=\delta_{m,0}\sum_n G_n^R(\zeta,\theta,\omega), \tag{54}$$

where we can see that every mode of Green's function *equally* contributes to $\tilde{G}^R$.

B. ac field

For the ac field, which is one of the key questions in the present paper, Green's function has a more complicated θ dependence. To evaluate the gauge-invariant Green's function (52), here we expand the original Green's function with respect to $eA(t)$ in a Taylor series: $G_n^R(\zeta,\theta+\int d\lambda eA,\omega)=\sum_\ell\frac{1}{\ell!}(\int d\lambda eA)^\ell\partial_\theta^\ell G_n^R(\zeta,\theta,\omega)$. Then the Wigner representation of the gauge-invariant Green's function is expressed as

$$\begin{aligned}\tilde{G}_m^R(\zeta,\theta,\omega)=\sum_{\ell n}\frac{2A^\ell}{\ell!\,\Omega}\int d\omega'\partial_\theta^\ell G_n^R(\zeta,\theta,\omega')\\ \times X_{m-n}^{(\ell)}Y^{(\ell)}\left(\frac{2}{\Omega}(\omega-\omega')\right),\end{aligned} \tag{55}$$

where

$$X_{m-n}^{(\ell)}\equiv\int_{-\pi}^{\pi}\frac{dx}{2\pi}e^{i(m-n)x}\sin^\ell x=\frac{1}{(2i)^\ell}\sum_{r=0}^{\ell}\binom{\ell}{r}(-1)^r\delta_{m-n,2r-\ell}, \tag{56}$$

and

$$\begin{aligned}Y^{(\ell)}(k)\equiv\int_{-\infty}^{\infty}\frac{dx}{2\pi}e^{ikx}\left(\frac{\sin x}{x}\right)^\ell=\frac{1}{2^\ell(\ell-1)!}\sum_{r=0}^{\ell}\binom{\ell}{r}(-1)^r\\ \times(k+\ell-2r)^{\ell-1}\theta(k+\ell-2r)\end{aligned} \tag{57}$$

for $\ell\geq 1$. When $\ell=0$, we have $Y^{(\ell)}(k)=\delta(k)$. The Floquet representation of Eq. (55) reads

$$\begin{aligned}\tilde{G}_{mn}^R(\zeta,\theta,\omega)=G_{mn}^R(\zeta,\theta,\omega)+\sum_{\ell=1}^{\infty}\frac{2}{\ell!\,\Omega}\left(\frac{A}{2i}\right)^\ell\sum_{r=0}^{\ell}(-1)^r\binom{\ell}{r}\\ \times\left(\int_{\omega}^{\Omega/2}d\omega'\sum_{k=0}^{\ell-1}+\int_{-\Omega/2}^{\omega}d\omega'\sum_{k=1}^{\ell}\right)\\ \times\partial_\theta^\ell G_{m-r+k,n+r+k-\ell}^R(\zeta,\theta,\omega')Y^{(\ell)}\\ \times\left(\frac{2}{\Omega}(\omega-\omega')-2k+\ell\right).\end{aligned} \tag{58}$$

The derivative with respect to θ in Eqs. (55) and (58) is simplified when the system is on the hypercubic lattice. The Floquet representation of the noninteracting Hamiltonian H is then given by Eq. (35), and the ℓth derivative of the Floquet representation of the retarded Green's function can be calculated for every ℓ via the recurrence relations

$$\partial_\theta H = \bar{H}, \tag{59}$$

$$\partial_\theta \bar{H} = -H, \tag{60}$$

$$\partial_\theta G^R = -G^R(-\partial_\theta H)G^R = G^R \bar{H} G^R. \tag{61}$$

Employing Eqs. (59)–(61) with relation (58), one can numerically evaluate the gauge-invariant retarded Green's function $\tilde{G}^R$ for the ac field.

VIII. APPLICATION TO THE FALICOV-KIMBALL MODEL

To test the ability of the present method for treating many-body systems, we apply it to the spinless FK model, for which the Hamiltonian is

$$H = -\sum_{ij} t_{ij} c_i^\dagger c_j + U \sum_i c_i^\dagger c_i f_i^\dagger f_i. \tag{62}$$

Here f_i ($f_i^\dagger$) annihilates (creates) a localized electron, and U is a coupling constant. It is known that the FK model exhibits a metal-insulator transition in infinite dimensions from DMFT calculations, where the possibility of charge-density wave phases is ignored.[14] The critical value of U for the transition is known to be $\sqrt{2}$ on the hypercubic lattice at half filling. The insulating phase is Mott-like, which means that the insulating state originates from the electron correlation.

What characterizes the FK model is that it has an exact solution for the impurity problem [Eq. (47)] within DMFT, even out of equilibrium.[29] The solution for the retarded Green's function is

$$G^R_{\mathrm{loc}}(\omega) = w_0 \mathcal{G}_0^R(\omega) + w_1 [\mathcal{G}_0^{R^{-1}}(\omega) - U]^{-1}, \tag{63}$$

where w_1 is the filling of the f electrons, and $w_0 = 1 - w_1$. Note that the retarded component of Green's function decouples to the Keldysh component. Here we concentrate on the retarded Green's function, and calculate the local spectral function $A_n(\omega) = -\frac{1}{\pi}\mathrm{Im}(G^R_{\mathrm{loc}})_n(\omega)$ (which is gauge invariant as explained in Sec. VII) and the gauge-invariant spectral function $\tilde{A}_n(\boldsymbol{k}, \omega) = -\frac{1}{\pi}\mathrm{Im}(\tilde{G}^R_{\boldsymbol{k}})_n(\omega)$ under the assumption that the initial correlations are irrelevant to the retarded Green's function.

A. Falicov-Kimball model in the dc field

We first present the results for the dc field. We start with noting that the integral over θ can be performed analytically due to relation (53), and that G^R_{loc}, $\mathcal{G}_0^R$, and Σ^R in the Floquet representation are all diagonal as mentioned in Sec. VII A, which simplifies our calculation. All the matrices we have to invert numerically are tridiagonal owing to Eq. (29).

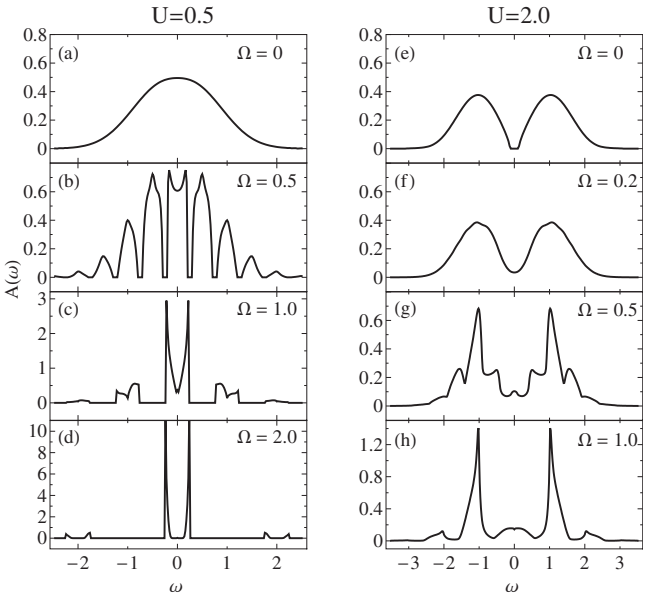

FIG. 4. The local spectral function $A_0(\omega)$ for the FK model coupled to the dc field on the hypercubic lattice at half filling.

In Fig. 4 we illustrate the local spectral function $A_0(\omega)$ for various values of U and Ω on the hypercubic lattice. The size of the Floquet matrices that we choose is typically 9–13. Convergence is achieved after typically 10–30 iterations, where the calculation is quite stable over the parameter space considered here. We can see that the present result in Figs. 4(b)–4(d) obtained in the Floquet method agrees well with the previous results,[33,35] where the nonequilibrium DMFT is employed. This suggests that our assumption of the irrelevance of the initial correlations to the retarded Green's function is valid. In our results, the spectral function is positive definite, and satisfies the sum rule for the zeroth spectral moment[36] as in equilibrium. Therefore we can safely interpret the quantity $A(\omega)$ as the spectrum of the system even out of equilibrium.

More interesting case is Figs. 4(e)–4(h), where we can observe how a Mott-like insulator ($U=2$) is driven into a metallic state by the dc field. Namely, while there is a clear band gap between the upper and lower bands in equilibrium [Fig. 4(e), $\Omega=0$], the gap disappears as the dc field is increased, where the spectral weight around $\omega=0$ develops. Hence our calculation captures the Mott-like insulator-to-metal transition induced by a static electric field. In the strong dc field region [Figs. 4(b)–4(d), 4(g), and 4(h)], we find complicated structures with the spacing Ω. We can attribute these to the Wannier-Stark ladder (mentioned in Sec. IV C 1), which grows with the field intensity $E \propto \Omega$ [see Eq. (24)]. The Wannier-Stark structure interferes with the original spectrum that comprises two bands with the spacing U, producing a characteristic interference pattern.

B. Falicov-Kimball model in the ac field

We move on to the ac field. While the spectral function is time independent for the dc field, i.e., the nonzeroth modes of $A_n(\omega)$ vanish, this is no longer the case for the ac field.

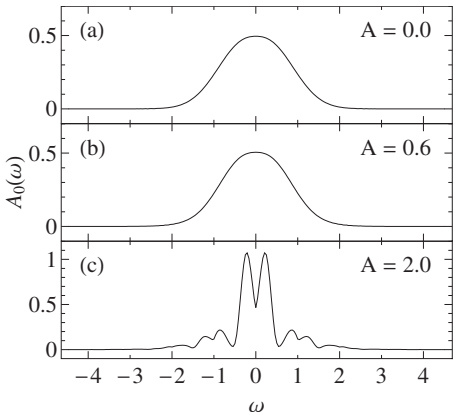

FIG. 5. The zeroth mode of the local spectral function $A_0(\omega)$ of the FK model coupled to the ac field ($\Omega=1$) on the hypercubic lattice at half filling for $U=0.5$.

Since our interest resides in the time-averaged spectral function $\int dt_{\mathrm{av}} A(\omega, t_{\mathrm{av}}) = A_0(\omega)$, we concentrate on the zeroth mode of the spectral function. Unlike the dc case the integral over θ is nontrivial, which has to be calculated numerically. In Figs. 5–8, we depict the local spectral function $A_0(\omega)$ on the hypercubic lattice at half filling with the frequency of the ac field $\Omega=1$. The efficiency of the convergence and the stability of the calculation are similar to the dc case.

In the metallic region (Fig. 5 for $U=0.5$ and Fig. 6 for $U=1.3$), one can see how the metallic spectrum of the system is deformed by the ac field. Namely, the width of the band shrinks with the intensity of the field. It can even goes to zero when A coincides with a zero of $J_0(A)$, which makes interacting electrons localize. This is quite similar to the noninteracting case as examined in Sec. IV C 2. Hence we have *the dynamical localization in interacting electron systems*. Note that the scaling of the bandwidth with $J_0(A)$ is a nonlinear effect of the ac field, as evident from $J_0(A)=1-(A/2)^2+\cdots$. The difference between noninteracting and interacting cases is that each peak in the dynamical Wannier-Stark ladder at $\omega=n\Omega$ $(n=0, \pm 1, \pm 2, \ldots)$ splits into two with the spacing U due to the correlation effect. This can clearly be seen in Fig. 5(c).

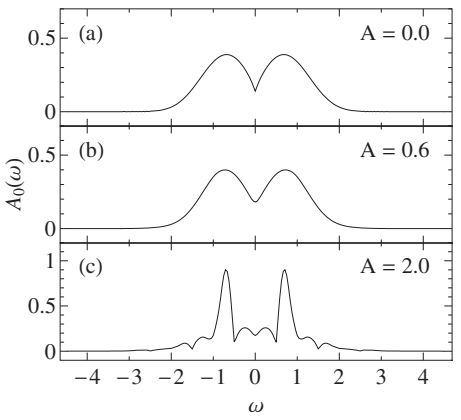

FIG. 6. The zeroth mode of the local spectral function $A_0(\omega)$ of the FK model coupled to the ac field ($\Omega=1$) on the hypercubic lattice at half filling for $U=1.3$.

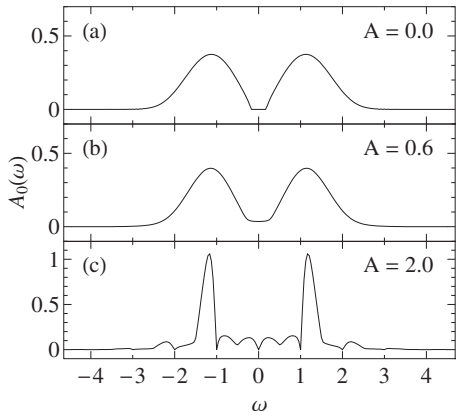

FIG. 7. The zeroth mode of the local spectral function $A_0(\omega)$ of the FK model coupled to the ac field ($\Omega=1$) on the hypercubic lattice at half filling for $U=2.2$.

In the insulating region (Fig. 7 for $U=2.2$ and Fig. 8 for $U=3.8$), on the other hand, we do observe the ac-field driven transition from the Mott-like insulating state to a metallic state. In equilibrium [Figs. 7(a) and 8(a)] the system has a gap between the upper and lower bands. When the ac field is switched on, the gap collapses [Figs. 7(b) and 8(b)], and a spectral weight grows in the midgap region around $\omega=0$. If we compare Figs. 7(b) and 8(b), we can see that the larger the band gap, the smaller the midgap weight. From these results, we see that metallic states appear in the insulating system of correlated electrons in the intense ac field. As the intensity of the ac field is further increased, the system plunges into the dynamical localization regime, where the bandwidth starts to scale with $J_0(A)$.

To characterize the metallic state, we have calculated the momentum resolved spectral function $\tilde{A}_0(\boldsymbol{k}, \omega)$. For clarity we take the simple cubic lattice with the JDOS [Eq. (E5)] in three dimensions. As a key result in the present paper, we plot the zeroth mode of the spectral function $\tilde{A}_0(\boldsymbol{k}, \omega)$ and $A_0(\omega)$ for the frequency $\Omega=1$ at half filling in Figs. 9 and 10, where we take $\boldsymbol{k}=k(1,1,1)$. One can check that the result respects the particle-hole symmetry. As discussed in Sec. VII B, numerical evaluation of $\tilde{A}_0(\boldsymbol{k}, \omega)$ is done in a pertur-

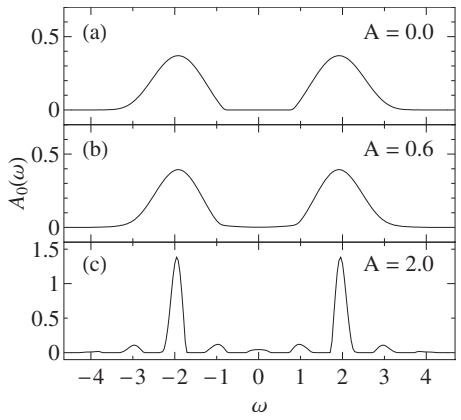

FIG. 8. The zeroth mode of the local spectral function $A_0(\omega)$ of the FK model coupled to the ac field ($\Omega=1$) on the hypercubic lattice at half filling for $U=3.8$.

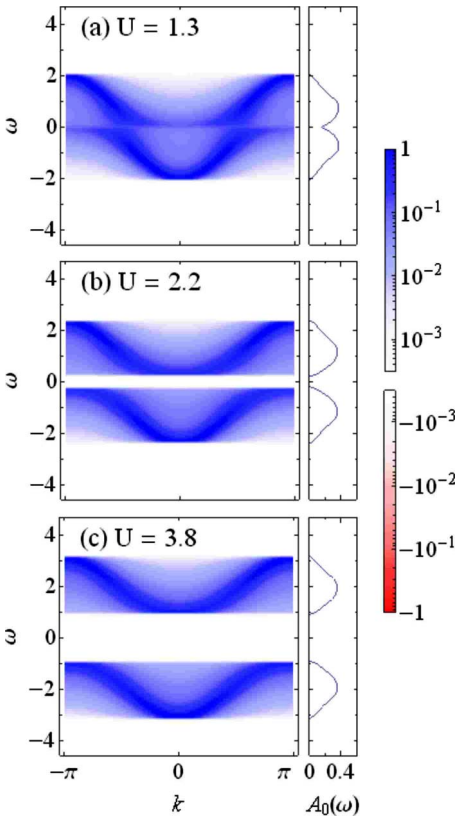

FIG. 9. (Color online) The zeroth mode of the gauge-invariant spectral function $\tilde{A}_0(\boldsymbol{k},\omega)$ with $\boldsymbol{k}=k(1,1,1)$ (the density plots) and the local spectral function $A_0(\omega)$ (the line plots) of the FK model coupled to the ac field ($\Omega=1$) on the simple cubic lattice at half filling for $A=0$ in units of t^*. The color bars on the right side represents the correspondence between the colors and the values of $\tilde{A}_0(\boldsymbol{k},\omega)$.

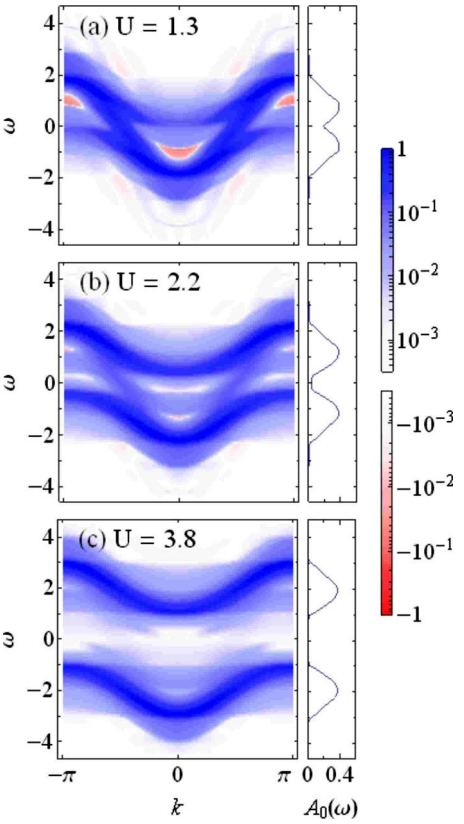

FIG. 10. (Color online) The zeroth mode of the gauge-invariant spectral function $\tilde{A}_0(\boldsymbol{k},\omega)$ with $\boldsymbol{k}=k(1,1,1)$ (the density plots) and the local spectral function $A_0(\omega)$ (the line plots) of the FK model coupled to the ac field ($\Omega=1$) on the simple cubic lattice at half filling for $A=0.6$ in units of t^*. The color bars on the right side represent the correspondence between the colors and the values of $\tilde{A}_0(\boldsymbol{k},\omega)$.

bative way. Thus we can obtain reliable results only in a weak intensity region. Although we use a perturbation in A, higher-order contributions are included in our calculations. To obtain the results in Figs. 9 and 10, the summation over ℓ in Eq. (58) is performed up to $\ell=5$. We have checked that the expansion in terms of A converges for $A \lesssim 0.6$. A calculation tends to be unstable when U is small ($\lesssim 1$) where the system is in a metallic state. When we analyze the results, we have to be careful with the sign of the spectral function $\tilde{A}_0(\boldsymbol{k},\omega)$. Although the local spectral function $A_0(\omega)$ is positive definite, $\tilde{A}_0(\boldsymbol{k},\omega)$ is not so in general. While we notice there are some regions where $\tilde{A}_0(\boldsymbol{k},\omega)$ becomes negative, the quantity is mostly positive for $A \lesssim 0.6$ and $U \gtrsim 2$. The result should be supported by other gauge-invariant quantities such as the current or the optical conductivity, which is a future problem.

First, let us see Figs. 9(a)–9(c). These are the spectra of the system in equilibrium ($A=0$). One can see how the metallic bands [Figs. 9(a)] change into the insulating ones [Figs. 9(b) and 9(c)] with a finite gap appearing with U. In the insulating state, the upper band is almost a replica of the lower one shifted upward by U, which is characteristic of the FK model. When the ac field is turned on in Figs. 10(a)–10(c) ($A=0.6$), we can see how the ac field generates a new *photoinduced band structure*. In Fig. 10(b), we can observe that a new band appears in the midgap region. This band is created by the electrons that absorb or emit one photon with the energy $\Omega=1$, that is, the photoinduced band is a replica of the original lower and upper bands shifted by Ω. If we assume that the states are occupied up to $\omega=0$ as in equilibrium, the electrons in the induced band around $\omega=0$ play a role of carriers, making the system metallic. When the interaction U is strong enough [Fig. 10(c), $U=3.8$], the metallic band does not appear. Instead, sidebands appear near the original bands with the spacing Ω in the midgap region. Again, the electrons in the sidebands consist of the electrons absorbing or emitting one photon with the energy Ω. Since Ω is much smaller than U here, the electrons cannot reach the region around $\omega=0$ with a one-photon process. Therefore the system remains to be insulating with the finite gap in the ac field. As well as the case of the dc field, the sideband pattern with the spacing Ω interferes with the original band structure with the spacing U, yielding complicated band patterns.

C. Relevance to experiments

Finally we mention the relevance of the present results to experiments. For the dc field, the intensity required for the

effect considered here is $\sim 10^{9-10}$ V/m for $a \sim 10^{0-1}$ Å, which is too strong to be realistic. However, in the case of the ac field, the required intensity is $A \sim 1$ [see Eq. (32)] for the dimensionless quantity, which translates to $E \sim 10^{9-10}$ V/m (i.e., the intensity of $\sim 10^{11-13}$ W/cm^2) for $\Omega \sim 1$ eV (visible light). For a smaller Ω the required intensity becomes smaller. Since the intensity of pulsed laser available with recent advances in optical techniques reaches such magnitudes,[37] it should be possible to observe the nonlinear effects predicted in this paper in experiments. One problem is that when the intensity goes beyond $\sim 10^{12}$ W/cm^2, atoms begin to be ionized and evaporated. To make the required field intensity smaller, we can take systems with large lattice constants, such as the zeolites loaded with guest atoms.[38] As an entirely different class of systems, we can consider cold atoms in optical lattices,[39] which may be an interesting playing ground for the effects examined in the present paper.

IX. CONCLUSION

We have developed a theoretical method to formulate photoinduced phenomena in correlated electron systems. The method incorporates FGFM into DMFT, which can fully take into account both the electron correlation effect and the nonlinear electric-field effect. We have applied the method to the Falicov-Kimball model in ac fields to calculate the gauge-invariant spectral functions. We find peculiar photoinduced band structures, which arise from the nonlinear effect of the electric field. In particular, we find a metallic state in the midgap region of the Mott-like insulator induced by the ac field. In the calculation we have utilized a theorem, found here, that identifies eigenvalues and eigenvectors of a Floquet matrix for single-band noninteracting electrons.

We believe that our approach has a potential ability to treat, not only the FK model considered in the paper, but also a wide class of models such as the Hubbard model. There are some future problems: one is to calculate the Keldysh component of Green's function G^K. We need the Keldysh Green's function to compute, e.g., the current or the optical conductivity which has information of the transport properties of the system. An application to the Hubbard model is also desirable. Experimentally, the relaxation of photoinduced states after the ac field is switched off is also an important phenomenon. This is theoretically interesting as well, for which further developments on the nonequilibrium DMFT would be necessary.

ACKNOWLEDGMENTS

This work was supported in part by a Grant-in-Aid for Scientific Research on a Priority Area "Anomalous quantum materials" from the Japanese Ministry of Education. N.T. was supported by the Japan Society for the Promotion of Science.

APPENDIX A: MULTIPLICATION RULE FOR THE FLOQUET MATRICES

Here we show that Floquet matrices obey the multiplication rule in the linear algebra. Let us prepare two functions $A(t,t')$ and $B(t,t')$ which satisfy the periodicity condition: $A(t+\tau,t'+\tau)=A(t,t')$ (and so does B). We write the following integral in the Wigner representation:

$$\begin{aligned}
\int dt'' A(t,t'')B(t'',t') &= \int dt'' \sum_{\ell} \int \frac{d\omega}{2\pi} e^{-i\omega(t-t'')-i\ell\Omega(t+t'')/2} A_{\ell}(\omega) \sum_{\ell'} \int \frac{d\omega'}{2\pi} e^{-i\omega'(t''-t')-i\ell'\Omega(t''+t')/2} B_{\ell'}(\omega') \\
&= \sum_{\ell\ell'} \int \frac{d\omega}{2\pi} \int \frac{d\omega'}{2\pi} 2\pi\delta\left(\omega-\omega'-\frac{\ell+\ell'}{2}\Omega\right) e^{-i\omega t-i\ell\Omega t/2+i\omega' t'-i\ell'\Omega t'/2} A_{\ell}(\omega) B_{\ell'}(\omega') \\
&= \sum_{\ell\ell'} \int \frac{d\omega}{2\pi} e^{-i\omega t-i\ell\Omega t/2+i[\omega-(\ell+\ell')\Omega/2]t'-i\ell'\Omega t'/2} A_{\ell}(\omega) B_{\ell'}\left(\omega-\frac{\ell+\ell'}{2}\Omega\right) \\
&= \sum_{\ell\ell'} \int \frac{d\omega}{2\pi} e^{-i(\omega-\ell'\Omega/2)(t-t')-i(\ell+\ell')\Omega(t+t')/2} A_{\ell}(\omega) B_{\ell'}\left(\omega-\frac{\ell+\ell'}{2}\Omega\right).
\end{aligned}$$

Thus we have

$$(AB)_k(\omega) = \sum_{\ell+\ell'=k} A_{\ell}\left(\omega+\frac{\ell'}{2}\Omega\right) B_{\ell'}\left(\omega-\frac{\ell}{2}\Omega\right).$$

Let us take an integer k' satisfying the condition $k' \equiv k \pmod 2$. Replacing ω with $\omega+k'\Omega/2$ gives

$$\begin{aligned}
(AB)_k\left(\omega+\frac{k'}{2}\Omega\right) = \sum_{\ell+\ell'=k} & A_{\ell}\left(\omega+\frac{k'+\ell'}{2}\Omega\right) \\
& \times B_{\ell'}\left(\omega+\frac{k'-\ell}{2}\Omega\right). \qquad \text{(A1)}
\end{aligned}$$

If we write Eq. (A1) in the Floquet representation following its definition (7), we arrive at the conclusion,

$$(AB)_{(k+k')/2,(k'-k)/2}(\omega) = \sum_{\ell} A_{(k+k')/2,(k+k')/2-\ell}(\omega) B_{(k+k')/2-\ell,(k'-k)/2}(\omega),$$

or a more transparent expression,

$$(AB)_{mn}(\omega) = \sum_{m'} A_{mm'}(\omega) B_{m'n}(\omega),$$

where $m=(k+k')/2$, $n=(k'-k)/2$, and $m'=(k+k')/2-\ell$, all of which are integers due to $k \equiv k'$ (mod 2). This ensures that we can apply the usual multiplication rule of a matrix to every Floquet-represented function.

APPENDIX B: DERIVATION OF THE FLOQUET REPRESENTATION OF THE NONINTERACTING GREEN'S FUNCTION

Here we derive the Floquet representation [Eq. (13)] of Green's function. Let us start with Eq. (12). We find that the argument of the exponential in Eq. (12) is not invariant under discrete translation against $t_{\rm rel}$. To somehow make it invariant under such a translation, we rewrite Eq. (12) into

$$G^{R0}_{\boldsymbol{k}}(t,t') = -i\theta(t_{\rm rel}) e^{it_{\rm rel}[\mu-(\epsilon_{\boldsymbol{k}})_0]} \times \exp\left(-i \int_{t_{\rm av}-t_{\rm rel}/2}^{t_{\rm av}+t_{\rm rel}/2} dt'' [\epsilon_{\boldsymbol{k}-e\boldsymbol{A}(t'')} - (\epsilon_{\boldsymbol{k}})_0] \right). \tag{B1}$$

Here $(\epsilon_{\boldsymbol{k}})_0$ is defined in Eq. (14). Now that the argument of the exponential in Eq. (B1) is periodic in $t_{\rm rel}$ with the period 2τ and in $t_{\rm av}$ with the period τ, we can insert the factors $\sum_\ell e^{-i\ell\Omega t_{\rm rel}/2} \frac{1}{2\tau} \int_{-\tau}^{\tau} dt'_{\rm rel} e^{i\ell\Omega t'_{\rm rel}/2}$ and $\sum_m e^{-im\Omega t_{\rm av}} \frac{1}{\tau} \int_{-\tau/2}^{\tau/2} dt'_{\rm av} e^{im\Omega t'_{\rm av}}$ into Eq. (B1). Then, with the Fourier-transformed expression of the step function,

$$\theta(t_{\rm rel}) = -\frac{1}{2\pi i} \int d\omega' \frac{e^{-i\omega' t_{\rm rel}}}{\omega' + i\eta}, \tag{B2}$$

where η is an infinitesimal positive constant, we can perform the Wigner transformation of Eq. (B1) as

$$(G^{R0}_{\boldsymbol{k}})_n(\omega) = \sum_{\ell m} \int \frac{d\omega'}{2\pi} \frac{1}{\omega' + i\eta} \int dt_{\rm rel} \frac{1}{\tau} \int_{-\tau/2}^{\tau/2} dt_{\rm av} e^{i[\omega+\mu-(\epsilon_{\boldsymbol{k}})_0-\omega'-\ell\Omega/2]t_{\rm rel}+i(n-m)\Omega t_{\rm av}} \times \frac{1}{2\tau} \int_{-\tau}^{\tau} dt'_{\rm rel} \frac{1}{\tau} \int_{-\tau/2}^{\tau/2} dt'_{\rm av} e^{i\ell\Omega t'_{\rm rel}/2+im\Omega t'_{\rm av}} \exp\left(-i \int_{t'_{\rm av}-t'_{\rm rel}/2}^{t'_{\rm av}+t'_{\rm rel}/2} dt'' [\epsilon_{\boldsymbol{k}-e\boldsymbol{A}(t'')} - (\epsilon_{\boldsymbol{k}})_0] \right). \tag{B3}$$

In order to make our notation clearer, we change the integral variables as $\Omega t'_{\rm rel}/2 = x'$, $\Omega t'_{\rm av} = y'$. After some calculations, we obtain

$$(G^{R0}_{\boldsymbol{k}})_n(\omega) = \sum_{\substack{\ell \equiv n \\ \text{mod } 2}} \frac{1}{\omega - \ell\Omega/2 + \mu - (\epsilon_{\boldsymbol{k}})_0 + i\eta} \times \int_{-\pi}^{\pi} \frac{dx'}{2\pi} \int_{-\pi}^{\pi} \frac{dy'}{2\pi} e^{i\ell x' + iny'} \times \exp\left(-\frac{i}{\Omega} \int_{y'-x'}^{y'+x'} dz [\epsilon_{\boldsymbol{k}-e\boldsymbol{A}(z/\Omega)} - (\epsilon_{\boldsymbol{k}})_0] \right). \tag{B4}$$

In the above we have used the fact that the integral in Eq. (B4) equals zero when $\ell \not\equiv n$ (mod 2) since $\iint dx'dy' = (\iint_{\rm I} + \iint_{\rm III}) + (\iint_{\rm II} + \iint_{\rm IV}) = [1+(-1)^{\ell+n}](\iint_{\rm I} + \iint_{\rm II})$, where the Roman numerals represent the ranges of the integral defined in Fig. 11. We further change the integral variables: $x'+y'=x$, $x'-y'=-y$. Here we have to be careful with the range of the integral. As shown in Fig. 11, we change the range of the integral from $\iint_{\square} dx'dy'$ to $\frac{1}{2}\iint_{\diamond} dx'dy'$, which is equal to $\frac{1}{2}\int_{-2\pi}^{2\pi} dx \int_{-2\pi}^{2\pi} dy$ times $\frac{1}{2}$ coming from the Jacobian. Then we change the range of the integral again: $\frac{1}{2} \times \frac{1}{2} \int_{-2\pi}^{2\pi} dx \int_{-2\pi}^{2\pi} dy = \int_{-\pi}^{\pi} dx \int_{-\pi}^{\pi} dy$. Note that the two $\frac{1}{2}$ factors are canceled out by the change of the range of the integral. As a consequence, we arrive at the general Wigner representation of Green's function,

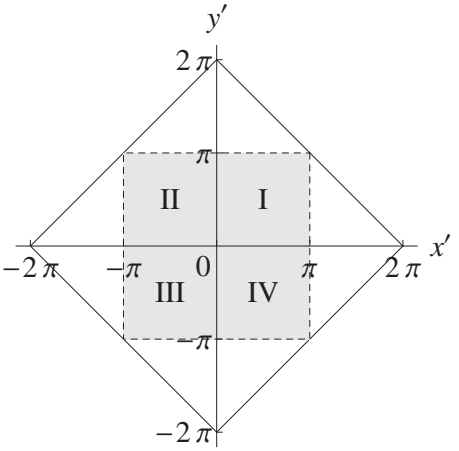

FIG. 11. The range of the integral: each Roman numeral denotes the corresponding shaded region, the symbols $\diamond$ and $\square$ used in the text denote the regions surrounded by the solid line and the broken line, respectively.

$$(G_{\boldsymbol{k}}^{R0})_n(\omega) = \sum_{\substack{\ell \equiv n \\ \text{mod } 2}} \frac{1}{\omega - \ell\Omega/2 + \mu - (\epsilon_{\boldsymbol{k}})_0 + i\eta} \times \int_{-\pi}^{\pi} \frac{dx}{2\pi} \int_{-\pi}^{\pi} \frac{dy}{2\pi} e^{i(\ell+n)x/2 - i(\ell-n)y/2} \times \exp\left(-\frac{i}{\Omega} \int_y^x dz [\epsilon_{\boldsymbol{k}-e\boldsymbol{A}(z/\Omega)} - (\epsilon_{\boldsymbol{k}})_0] \right). \tag{B5}$$

Next, let us move on to the Floquet representation. Following the definition of the Floquet representation [Eq. (4)], we have

$$(G_{\boldsymbol{k}}^{R0})_{mn}(\omega) = \sum_{\substack{\ell \equiv m-n \\ \text{mod } 2}} \frac{1}{\omega + (m+n-\ell)\Omega/2 + \mu - (\epsilon_{\boldsymbol{k}})_0 + i\eta} \times \int_{-\pi}^{\pi} \frac{dx}{2\pi} \int_{-\pi}^{\pi} \frac{dy}{2\pi} e^{i(\ell+m-n)x/2 - i(\ell-m+n)y/2} \times \exp\left(-\frac{i}{\Omega} \int_y^x dz [\epsilon_{\boldsymbol{k}-e\boldsymbol{A}(z/\Omega)} - (\epsilon_{\boldsymbol{k}})_0] \right).$$

In the above we can replace $m+n-\ell$ with 2ℓ due to $m+n-\ell \equiv m-n-\ell \equiv 0 \pmod 2$, which gives Eq. (13).

APPENDIX C: UNITARITY OF $\Lambda_{\boldsymbol{k}}$

We prove that $\Lambda_{\boldsymbol{k}}$ defined by Eq. (15) is a unitary matrix for any $\epsilon_{\boldsymbol{k}}$ and $\boldsymbol{A}(t)$ as

$$\begin{aligned} \sum_{\ell} (\Lambda_{\boldsymbol{k}})_{m\ell} (\Lambda_{\boldsymbol{k}}^{\dagger})_{\ell n} &= \int_{-\pi}^{\pi} \frac{dx}{2\pi} \int_{-\pi}^{\pi} \frac{dy}{2\pi} \sum_{\ell} e^{i(mx-ny)-i\ell(x-y)} \times \exp\left(-\frac{i}{\Omega} \int_y^x dz [\epsilon_{\boldsymbol{k}-e\boldsymbol{A}(z/\Omega)} - (\epsilon_{\boldsymbol{k}})_0] \right) \\ &= \int_{-\pi}^{\pi} \frac{dx}{2\pi} \int_{-\pi}^{\pi} dy\, \delta(x-y) e^{i(mx-ny)} \times \exp\left(-\frac{i}{\Omega} \int_y^x dz [\epsilon_{\boldsymbol{k}-e\boldsymbol{A}(z/\Omega)} - (\epsilon_{\boldsymbol{k}})_0] \right) \\ &= \int_{-\pi}^{\pi} \frac{dx}{2\pi} e^{i(m-n)x} = \delta_{mn}. \end{aligned}$$

Since $\Lambda_{\boldsymbol{k}}$ is nothing but a set of Floquet state vectors [Eq. (45)], this unitarity relation indicates that the Floquet states $u_{\boldsymbol{k}}^{m-n}$ form an orthonormal and complete basis.

APPENDIX D: INVERSE OF $G_{\boldsymbol{k}}^{R0}$

The inverse of $(G_{\boldsymbol{k}}^{R0})_{mn}(\omega)$ is calculated for any $\epsilon_{\boldsymbol{k}}$ and $\boldsymbol{A}(t)$ as follows. First, using expression (17) we have $G_{\boldsymbol{k}}^{R0^{-1}} = \Lambda_{\boldsymbol{k}} \cdot Q_{\boldsymbol{k}}^{-1}(\omega) \cdot \Lambda_{\boldsymbol{k}}^{\dagger}$ since $\Lambda_{\boldsymbol{k}}$ is unitary as proved in Appendix C. Among the terms in the diagonal matrix $Q_{\boldsymbol{k}}^{-1}(\omega)$, $[\omega + \mu - (\epsilon_{\boldsymbol{k}})_0 + i\eta]\delta_{mn}$ commutes with $\Lambda_{\boldsymbol{k}}$, giving a trivial result. The only nontrivial part, $n\Omega\delta_{mn}$, is evaluated as

$$\begin{aligned} \sum_{\ell} (\Lambda_{\boldsymbol{k}})_{m\ell} \ell\Omega (\Lambda_{\boldsymbol{k}}^{\dagger})_{\ell n} &= \int_{-\pi}^{\pi} \frac{dx}{2\pi} \int_{-\pi}^{\pi} \frac{dy}{2\pi} \sum_{\ell} e^{i(mx-ny)-i\ell(x-y)} \ell\Omega \exp\left(-\frac{i}{\Omega} \int_y^x dz [\epsilon_{\boldsymbol{k}-e\boldsymbol{A}(z/\Omega)} - (\epsilon_{\boldsymbol{k}})_0] \right) \\ &= \int_{-\pi}^{\pi} \frac{dx}{2\pi} \int_{-\pi}^{\pi} dy i\Omega [\partial_x \delta(x-y)] e^{i(mx-ny)} \exp\left(-\frac{i}{\Omega} \int_y^x dz [\epsilon_{\boldsymbol{k}-e\boldsymbol{A}(z/\Omega)} - (\epsilon_{\boldsymbol{k}})_0] \right) \\ &= \int_{-\pi}^{\pi} \frac{dx}{2\pi} \int_{-\pi}^{\pi} dy\, \delta(x-y) [m\Omega - \epsilon_{\boldsymbol{k}-e\boldsymbol{A}(x/\Omega)} + (\epsilon_{\boldsymbol{k}})_0] e^{i(mx-ny)} \exp\left(-\frac{i}{\Omega} \int_y^x dz [\epsilon_{\boldsymbol{k}-e\boldsymbol{A}(z/\Omega)} - (\epsilon_{\boldsymbol{k}})_0] \right) \\ &= [m\Omega + (\epsilon_{\boldsymbol{k}})_0] \delta_{mn} - (\epsilon_{\boldsymbol{k}})_{m-n}. \end{aligned} \tag{D1}$$

Between the second and the third lines we have integrated by parts. The contribution coming from the boundary is negligible due to the presence of the delta function. Thus the simple expression [Eq. (18)] results.

We note that relation (D1) for the Floquet indices $m=n=0$ reduces to the geometrical phase, $\gamma_{\boldsymbol{k}} = \int_{-\pi/2}^{\pi/2} dt u_{\boldsymbol{k}}^{*}(t) i\partial_t u_{\boldsymbol{k}}(t)$. From Eq. (D1), we can show that it is exactly absent in the single-band noninteracting system, $\gamma_{\boldsymbol{k}} = -2\pi \Sigma_{\ell} \ell (\Lambda_{\boldsymbol{k}})_{0\ell} (\Lambda_{\boldsymbol{k}}^{\dagger})_{\ell 0} = 0$.

APPENDIX E: JOINT DENSITY OF STATES IN ARBITRARY FINITE DIMENSIONS

An analytic expression for JDOS defined by Eq. (22) can be obtained in arbitrary dimensions. We first substitute the delta functions in Eq. (22) with the integrals over auxiliary variables s and $\bar{s}$:

$$\rho(\epsilon, \bar{\epsilon}) = \int_{-\infty}^{\infty} \frac{ds}{2\pi} \int_{-\infty}^{\infty} \frac{d\bar{s}}{2\pi} e^{is\epsilon + i\bar{s}\bar{\epsilon}} \sum_{\boldsymbol{k}} e^{2it\Sigma_i (s \cos k_i + \bar{s} \sin k_i)}.$$

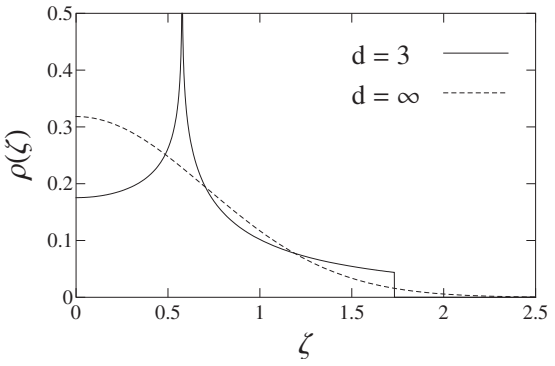

FIG. 12. The JDOS $\rho(\zeta)$ for $d=3$ and $d=\infty$ in units of t^*.

We then replace ϵ and $\bar{\epsilon}$ with ζ and θ in accordance with $\epsilon=\zeta\cos\theta$ and $\bar{\epsilon}=\zeta\sin\theta$, and change the integral variables as $s=\xi\sin\phi$ and $\bar{s}=\xi\cos\phi$. After the integrations, we obtain

$$\rho(\zeta)=\int_0^\infty \frac{d\xi}{2\pi}\xi J_0(\zeta\xi)[J_0(2t\xi)]^d. \tag{E1}$$

This is the general expression for the JDOS in d dimensions. Note that the JDOS is independent of θ in any dimension. The infinite-dimensional case is readily reproduced since $J_0(z)=1-(z/2)^2+O(z^4)$ and $t=t^*/2\sqrt{d}$, the factor $[J_0(2t\xi)]^d$ converges to $e^{-(\xi/2)^2}$ in the limit $d\to\infty$. With a formula for the integral of the Bessel function, we reproduce the known JDOS in infinite dimensions:[22]

$$\rho_{d=\infty}(\zeta)=\frac{1}{\pi}e^{-\zeta^2}. \tag{E2}$$

In the case of finite dimensions, we can systematically deduce the JDOS from Eq. (E1) with an appropriate integral formula related to the Bessel function. In the following we list the derived expression of the JDOS for $d=1,2,3$:

$$\rho_{d=1}(\zeta)=\frac{1}{2\pi(2t)}\delta(\zeta-2t), \tag{E3}$$

$$\rho_{d=2}(\zeta)=\begin{cases}\dfrac{1}{\pi^2\zeta\sqrt{4(2t)^2-\zeta^2}}, & 0<\zeta<4t\\ 0, & 4t<\zeta,\end{cases} \tag{E4}$$

$$\rho_{d=3}(\zeta)=\begin{cases}\dfrac{2}{\pi^3\sqrt{(\zeta+2t)^3(6t-\zeta)}}K\left(4\sqrt{\dfrac{(2t)^3\zeta}{(\zeta+2t)^3(6t-\zeta)}}\right), & 0\le\zeta<2t\\ \dfrac{1}{2\pi^3\sqrt{(2t)^3\zeta}}K\left(\dfrac{1}{4}\sqrt{\dfrac{(\zeta+2t)^3(6t-\zeta)}{(2t)^3\zeta}}\right), & 2t<\zeta\le 6t\\ 0, & 6t<\zeta,\end{cases} \tag{E5}$$

where $K(k)$ is the elliptic integral of the first kind. In Fig. 12 we plot the JDOS for $d=3$ and $d=\infty$. We can observe that $\rho_{d=3}$ diverges at $\zeta=2t$, which originates from the van Hove singularity of the simple cubic lattice.

[1] K. Nasu, Rep. Prog. Phys. **67**, 1607 (2004).
[2] Y. Tokura, J. Phys. Soc. Jpn. **75**, 011001 (2006).
[3] K. Miyano, T. Tanaka, Y. Tomioka, and Y. Tokura, Phys. Rev. Lett. **78**, 4257 (1997).
[4] M. Fiebig, K. Miyano, Y. Tomioka, and Y. Tokura, Science **280**, 1925 (1998).
[5] M. Matsubara, Y. Okimoto, T. Ogasawara, Y. Tomioka, H. Okamoto, and Y. Tokura, Phys. Rev. Lett. **99**, 207401 (2007).
[6] R. Kubo, J. Phys. Soc. Jpn. **12**, 570 (1957).
[7] We basically follow N. Tsuji, M.S. thesis, University of Tokyo, 2008.
[8] F. H. M. Faisal, Comput. Phys. Rep. **9**, 55 (1989).
[9] S. C. Althorpe, D. J. Kouri, D. K. Hoffman, and N. Moiseyev, Chem. Phys. **217**, 289 (1997).
[10] T. Brandes and J. Robinson, Phys. Status Solidi B **234**, 378 (2002).
[11] D. F. Martinez, J. Phys. A **36**, 9827 (2003).
[12] A. Georges, G. Kotliar, W. Krauth, and M. J. Rozenberg, Rev. Mod. Phys. **68**, 13 (1996).
[13] L. M. Falicov and J. C. Kimball, Phys. Rev. Lett. **22**, 997 (1969).
[14] J. K. Freericks and V. Zlatić, Rev. Mod. Phys. **75**, 1333 (2003).
[15] A. V. Joura, J. K. Freericks, and T. Pruschke, Phys. Rev. Lett. **101**, 196401 (2008).
[16] J. H. Shirley, Phys. Rev. **138**, B979 (1965).
[17] H. Sambe, Phys. Rev. A **7**, 2203 (1973).
[18] T. Dittrich, P. Hänggi, G.-L. Ingold, B. Kramer, G. Schön, and W. Zwerger, *Quantum Transport and Dissipation* (Wiley-VCH, Weinheim, 1998).
[19] G. Floquet, Ann. Sci. Ec. Normale Super. **12**, 47 (1883).
[20] J. Schwinger, J. Math. Phys. **2**, 407 (1961).
[21] L. V. Keldysh, Zh. Eksp. Teor. Fiz. **47**, 1515 (1965) [Sov. Phys. JETP **20**, 1018 (1965)].
[22] V. Turkowski and J. K. Freericks, Phys. Rev. B **71**, 085104 (2005).
[23] D. H. Dunlap and V. M. Kenkre, Phys. Rev. B **34**, 3625 (1986).

[24] E. Müller-Hartmann, Z. Phys. B: Condens. Matter **74**, 507 (1989); note the difference of the factor $\sqrt{2}$ in definition (36) from this reference.
[25] A. P. Jauho and K. Johnsen, Phys. Rev. Lett. **76**, 4576 (1996).
[26] K. B. Nordstrom, K. Johnsen, S. J. Allen, A.-P. Jauho, B. Birnir, J. Kono, T. Noda, H. Akiyama, and H. Sakaki, Phys. Rev. Lett. **81**, 457 (1998).
[27] A. Georges and G. Kotliar, Phys. Rev. B **45**, 6479 (1992).
[28] W. Metzner and D. Vollhardt, Phys. Rev. Lett. **62**, 324 (1989).
[29] J. K. Freericks, V. M. Turkowski, and V. Zlatić, Phys. Rev. Lett. **97**, 266408 (2006).
[30] M. Eckstein and M. Kollar, Phys. Rev. Lett. **100**, 120404 (2008).
[31] P. Schmidt and H. Monien, arXiv:cond-mat/0202046 (unpublished).
[32] D. G. Boulware, Phys. Rev. **151**, 1024 (1966).
[33] V. Turkowski and J. K. Freericks, *Strongly Correlated Systems, Coherence and Entanglement* (World Scientific, Singapore, 2007).
[34] We cannot apply the assumption to the Keldysh component of the Green's function according to M.-T. Tran, Phys. Rev. B **78**, 125103 (2008).
[35] J. K. Freericks, Phys. Rev. B **77**, 075109 (2008).
[36] V. M. Turkowski and J. K. Freericks, Phys. Rev. B **73**, 075108 (2006).
[37] G. A. Mourou, T. Tajima, and S. V. Bulanov, Rev. Mod. Phys. **78**, 309 (2006).
[38] For instance, alkali-metal loaded zeolite is suggested to be a strongly correlated system by R. Arita, T. Miyake, T. Kotani, M. van Schilfgaarde, T. Oka, K. Kuroki, Y. Nozue, and H. Aoki, Phys. Rev. B **69**, 195106 (2004).
[39] O. Morsch and M. Oberthaler, Rev. Mod. Phys. **78**, 179 (2006).